

**CHEMICAL TRANSPORT REACTION OF THE COMPOUNDS
SmSe AND SmTe USING IODINE AS A TRANSPORT AGENT**

**A THESIS SUBMITTED TO THE SCHOOL OF GRADUATE
STUDIES IN PARTIAL FULFILMENT OF THE REQUIREMENT
FOR THE DEGREE OF MASTER OF SCIENCE IN CHEMISTRY**

BY ABI TADDESSE

JUNE 1998

*Listen to the glad shouts of victory
in the tents of God's people:
"The LORD'S mighty power has done it"
ps 118 : 15*

ACKNOWLEDGEMENT

First and foremost praise be to the Almighty God; the cherisher, the sustainer and the governor of the worlds, for allowing me to acknowledge those who directly or indirectly contribute their part to make me successful during my study.

My advisor, Dr. Veit Marx deserves a very special acknowledgement for his unreserved help in giving thoughtful suggestions, valuable comments and consistent encouragement in achieving my goal. His support in availing different reference materials and particularly regarding the arrangement of a computer with its full accessories is very greatly acknowledged.

I am thankful to my Co-advisor Dr. Negusse Retta for his constructive advice and thoughtful comments.

I feel a debt of gratitude for all the staffs of the department of chemistry. Among them I am particularly indebted to Ato Wodage Emiru and Ato Fikru for their unreserved help in designing the reactor. I wish to thank Dr. Girma Moges and Dr. Chandravanshi for availing their laboratory in time of my need. I wish also to thank Dr. Bernd Hundhammer for his supportive comments during the furnace construction.

It is a pleasure to acknowledge the help afforded me by Prof. T. Petzel, Mr. B. Hormann and Mr. H.J. Hertzner for analysing my samples.

I would like to express my deepest appreciation to my colleagues as a whole. Special thanks goes to W/o Tsige Bayisa, W/o Aziza Ahmed, W/t Emmebet Alemu, Ato Haile Mulesa, Ato Belayhun Keskes and Ato Solomon Hailu for their friendly assistance both morally and materially during the entire period. Highest praise and commendation goes to

Ato Sani Mussa, Ato Tezera Worku and Ato Tesema Worku for their constructive support in designing the furnace outer parts and W/o Ehitu Gezahegne and W/o Hirut for their unreserved help in photocopying the necessary articles and the thesis itself.

At last but not least, my factory (Addis Glass Factory) is very greatly acknowledged for granting me the opportunity and sponsorship to study for a higher degree.

CONTENTS

	Page
Acknowledgements	i
Table of Contents	iii
List of Figures	vi
List of Tables	vii
List of Appendices	ix
Abstract	x
1. INTRODUCTION	
1.1 Crystal Growth from the Vapour	1
1.1.1 General	1
1.1.2 Scope of Application	4
1.1.3 Factors Affecting Crystal Growth by CTR	5
1.1.3.1 The Nature and Selection of the Transport Agent	5
1.1.3.2 Concentration of the Transport Agent	7
1.1.3.3 Geometry of the Tube	8
2. LITERATURE REVIEW	
2.1 Rare - Earth Chalcogenides	10
2.1.1 Oxidation State	10
2.1.2 Crystallographic Structures	11
2.2 Formation of Rare - Earth Monoselenides	11
2.2.1 Preparation of Polycrystals	11
2.2.2 Formation of Single Crystals	13

2.3 Formation of Rare - Earth Monotellurides	14
2.3.1 Formation of Polycrystals	14
2.3.2 Preparation of Single Crystals	14
3. THERMODYNAMICS	
3.1 Thermochemical Calculations	16
3.2 The Program	20
3.3 Selection of Optimum Operating Conditions	21
3.3.1 Transport of SmS with Iodine	21
3.3.2 Transport of SmS with Bromine	22
3.3.3 Transport of SmSe with Bromine	23
3.3.4 Transport of SmSe with Iodine	23
3.3.5 Transport of SmTe with Bromine	24
3.3.6 Transport of SmTe with Iodine	25
3.4 Conclusion of the Calculation	26
4. EXPERIMENTAL	
4.1 Construction of the Transport Oven	27
4.2 Preparation of the Quartz Glass Tube	28
4.3 Synthesis of the Samarium Selenide Powder	29
4.4 Synthesis of the Samarium Telluride Powder	30
4.5 Optimization of the Furnace	30
4.6 Chemical Transport of SmTe	32
4.7 Chemical Transport of SmSe	33

5. Characterization of Products by X-ray	
powder Diffraction Technique	
5.1 Principles and Uses of Powder Diffraction Method	34
5.2 Measurement of Powder Diffraction Pattern	35
5.3 Characterization of Products by Guinier Powder Diffraction Method	36
6. RESULTS AND DISCUSSIONS.	42
7. CONCLUSIONS	51
8. REFERENCES	52
9. APPENDICES	57

LIST OF FIGURES

Figure	Page
1. Growth by Chemical Transport Reaction	3
2. A Model Showing the Ideal Boundary of the Reactor	16
3. Tubular Refractory Furnace	27
4. Temperature Distribution in the Furnace : Tap Position 13% and the Furnace one Side Open	32
5. Temperature Distribution in the Furnace :Tap Position 10% and the Furnace one Side Open	33

LIST OF TABLES

Table	Page
1. Some Thermodynamic Data Used in the Computation of the Reactions Given in Section 3.1	17
2. Temperature Distribution of the Furnace for Tap Position 13%	31
3. Temperature Distribution of the Furnace for TAP position 10%	32
4. X - ray Data for SmSe Raw - Material	36
5. X - ray Data for SmSe Residue	37
6. X - ray Data for SmSe Transport	37
7. X - ray Data for SmTe Raw - Material	37
8. X - ray Data for SmTe Residue	38
9. X - ray Data for SmTe Transport	38
10. X - ray Data for Sm ₂ O ₂ Se / SmSe Raw - Material	39
11. X - ray Data for Sm ₂ O ₂ Se/ SmSe Residue	39
12. X - ray Data for Sm ₂ O ₂ Se/ SmSe Transport	40
13. X - ray Data for Sm ₃ Se ₄ / SmSe Raw - Material	40
14. X - Ray Data for Sm ₃ Se ₄ / SmSe Residue	41
15. X - ray Data for Sm ₃ Se ₄ / SmSe Transport	41
16. Optimum Operating Conditions for both SmSe and SmTe	44
17. X - ray Data Showing a Comparison between the Standard and the Prepared SmSe	44
18. X - ray Data Showing a Comparison between the Standard and the Prepared SmTe	45

19. Growth time of Some Compounds	46
20. X - ray Data Comparing the Compound Sm_3Se_4 with the Standard	47
21. X - ray Data Comparing the Compound $\text{Sm}_2\text{O}_2\text{Se}$ with the Standard	48

ABSTRACT

Chemical transport reaction in a temperature gradient is used to grow single crystals of SmSe and SmTe in a closed tube using a one side open tubular furnace built by us.

Chemical transport of these two compounds is achieved using iodine as a transport agent.

The optimum operating conditions which are basically predicted by thermodynamics and as positively observed by experiment are $T_s = 668$ °K and $T_d = 475$ °K for the system SmSe / I₂ and $T_s = 717$ °K and $T_d = 503$ °K for the System SmTe / I₂ .

Better transport rate is observed for the system SmTe / I₂ . However , the sizes of the crystals grown in both cases are relatively small owing to the relatively shorter time that the reactors stayed in the furnace.

As one of the prime objectives of chemical transport reaction is separation of the compound of interest from other impurities that is cleaning , this is observed for the system SmSe / I₂ which separates itself from the compound Sm₃Se₄ .

LIST OF APPENDICES

APPENDIX	Page
1 . Listing of Pascal Program	57-I
2. Diagrams showing results of thermochemical calculations that are used in identifying the optimum operating conditions	57-II
3. Graph showing the temperature distribution in the furnace in different conditions and various taps.	57-III

1. INTRODUCTION

1.1 Crystal Growth from the Vapour

1.1.1 General

The method of crystal growth from the vapour phase is mainly used to obtain single crystal platelets (1), thin crystal layers (films) and metal whiskers (2) and the growth of certain organic crystals (3). An advantage of growth from the vapour is that in some cases extremely pure crystals with good surfaces are produced.

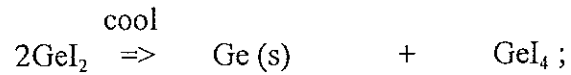
Crystallisation from the vapour phase can be classified in to three main categories (4). These are growth by *sublimation, chemical vapour deposition, and chemical transport reaction.*

Growth by *sublimation* :- In the simplest case the material to be crystallised is evaporated at a sufficiently high temperature, and the vapour is then led to a region of lower temperature where it crystallises by condensation. The direction of transport in this technique is always from hot to cold. The important conditions that must be fulfilled are a thermodynamic equilibrium should be established between the solid and the gas phase and the vaporisation has to be congruent i.e. the composition in the solid and the gas phase has to be the same. Crystal growth in this technique especially for rare-earth compounds requires relatively higher temperature for most of these compounds exhibit very high vaporisation points.

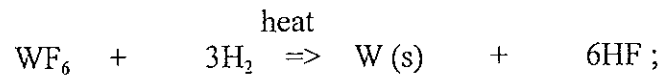
Chemical Vapour Deposition (CVD) :- In growth by this technique, the feed vapours must be generated by evaporation from a surface, usually a solid surface. The volatilized material then is transported to a substrate on which it is decomposed (5). In most cases, the deposition substrate must be kept at a relatively high temperature although in very rare cases

the opposite may happen. This chemical transformation may generally be achieved by processes of the following type :

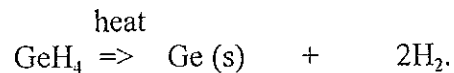
- disproportionation of high temperature species, e.g.:



- reduction, e.g.:



- pyrolysis, e.g.:



Chemical Transport Reaction (CTR) :- This applies to reactions in which a solid source material reacts with a gaseous transport agent at a temperature T_1 to produce exclusively gaseous products, while at another location in the system at temperature T_2 the reverse reaction occurs resulting in the deposition of the material to be crystallised (7,8).

Chemical transport reaction is similar to sublimation except that a carrier gas, often a halogen, is present to help volatilize the non-volatile metal component (9), and the direction of transport in the former case is not only in one direction (hot→cold) but also the reverse is possible.

Chemical transport reaction differs from that of chemical vapour deposition in that in the first case the carrier gas acts as a catalyst transporting the compound of interest to the place of deposition but is not finally involved in the process. In the second case, the reagents are changed during the course of reaction (6).

Chemical transport reactions are usually performed in evacuated quartz ampoules which are placed in a gradient furnace (4). In a closed system the transport direction is dependent upon the thermodynamic properties of the transport reaction.

In the simplest cases the reaction is demonstrated by the following scheme:



where A denotes the material to be crystallised, B, C, and D denote the other materials participating in the reaction and a, b, c and d are stoichiometrical ratios. The zone of the system where the reaction proceeds from left to right is the source, where as the zone where the reaction takes place from right to left is the zone of crystallisation. Schematically, chemical transport reaction can be described as depicted in the fig -1 below.

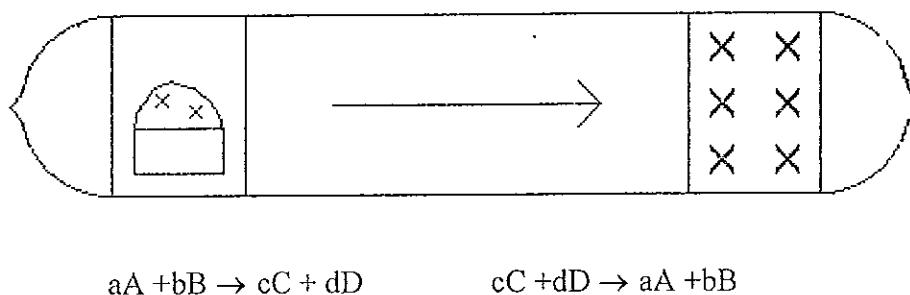


Fig 1. Growth by chemical transport reaction

In every case of crystal growth from the vapour, the vaporised material must be transported to the place of crystallisation. A simple method of transport is diffusion of the vaporised materials. Of course there are different modes of transport like for instance convection where the method of transport depends on the partial pressure of the transporter.

In general the direction of transport in chemical transport reaction depends on the nature of the reaction (6, 9 - 11). If the reaction is endothermic, where ΔH is positive, the

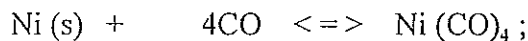
equilibrium is further to the right at higher temperatures, so that more products are formed in the hot region, and more reactants in the cold region. An endothermic reaction therefore, results in the transport from hot to cold, and an exothermic reaction where ΔH is negative, in the other hand results in the transport from cold to hot.

Needless to say, it is the sign of ΔH that determines the direction of the transport. It should be noted that if ΔH is zero, then there is no partial pressure difference along the temperature gradient, that is between the source and the product substrate or crystal, and therefore, no transport occurs.

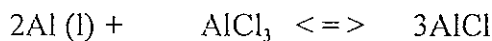
1.1.2 Scope of Application

The technique of chemical transport is widely used in the preparation of crystals and doped solids. Several chemical transport reactions of industrial interest include :

- the well - known Mond-Langer process which is widely used commercially to extract pure Ni crude metal containing other transition elements, i. e.,

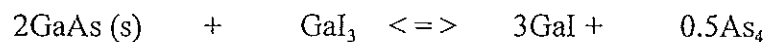


- the reaction



which has been seriously considered for Al purification, where Al (l) present initially in the crude alloy form ;

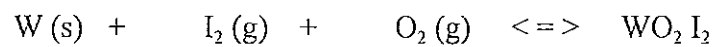
- the reaction



which can be used to prepare GaAs (s), a compound difficult to prepare by sublimation or melt growth. This compound is well - known for its use in the semiconductor industry.

The other application is that this process is also useful in theories of ore genesis and in the development of metal - halide lamps (6). For instance, the efficiency of converting

electricity to light with an increment filament life is a rapidly increasing function of temperature. The filament temperature is increased from 2800 to 3300 ° K, making the efficiency doubled. However, lamp life time decreases markedly with increasing temperature due to the presence of "hot spots" along the filament. Transport of tungsten can occur along the temperature gradient to the cooler parts of the filament. It has been found that halogen - containing additives can reverse this transport effect and there by increase the filament life time. The reaction responsible is the following :



1.1.3 Factors Affecting Crystal Growth by CTR

The important parameters affecting the quantity of the transported crystals include :

1. the source temperature
2. the temperature profile along the reaction tube
3. the nature and selection of the transporter.
4. concentration of the transport agent
5. geometry of the tube

From the above mentioned parameters, the source temperature and the temperature profile will be discussed in detail in the next section (see sec. 3.3). Now, we will concentrate on the remaining ones.

1.1.3.1 The nature and selection of transport agent

The substance that is used as a transport agent should exhibit the following properties.

- It must be stable in the gaseous form in the temperature range of interest.

- It shouldn't appear in the final product
- It should be easy to handle.

The exploratory work needed to achieve the desired result, when carried out in an empirical trial-and-error fashion, will often be ineffective and time consuming. The slowness of the empirical approach arises from the many experimental variables which can affect the results, coupled to the time needed to set up and run an experiment before it can be evaluated. Even when a useful system is known or can be guessed at from experience a good deal of experimentation may be necessary to obtain satisfactory results and optimise the conditions. There is obviously much to be gained when suitable solvent components and growth conditions can be chosen on a theoretical basis.

Theoretically, the nature and type of transport agent is studied based on (18 - 22) thermodynamic considerations. The transporter is expected to react with the compound to be transported at relatively lower temperature and should decompose easily in the reversible reaction without contaminating the deposited substance. The extent of contamination being dependent on the concentration of the carrier.

The most common transporting agents are halogens, iodine being the most easily employed one thanks to its solid nature at ambient temperature (23). For fluid transport agents, special apparatus is necessary to inject the materials in the reactor. This is because most of these compounds can not be easily managed during evacuation and sealing of the ampoule (24).

It should be stressed that theoretical predictions of transport rates can never fully replace practical studies although they may help to guide the planning of such experiments so that they can be carried out efficiently (25).

1.1.3.2 Concentration of the transport agent

Usually the effect of changing the temperature gradient and concentration of transport agent are to some extent similar. However, because of the risk of contaminating the crystal the aim is always to reduce the concentration of the transporter (26).

The contamination of the crystal by the transport agent was found to increase with the amount of the transport agent. Since growth rate increases accordingly, it is necessary to limit this amount at the expense of the size of crystals. Besides, an upper limit is set by the maximum allowable total pressure, but other consideration such as crystal quality, impurity incorporation, has to be taken into account (17).

The measured dependence of transport rate on transport agent concentration is dependent on the type of transport mode which also depends on the total pressure of the transporter. One should note that the total pressure created in the ampoule is considered as the pressure of the transport agent especially for rare earth monochalcogenides. Therefore, at low total pressures < 0.5 atm., the rate of transport increases linearly with increasing pressure which indicates that the heterogeneous solid- gas equilibria, either at T_s and / or at T_d are the rate determining steps where T_s and T_d are the source and deposition temperatures respectively . In the pressure intervals $0.5 - 1.5$ atm., the flux varies inversely with increasing pressure which indicates that the transport is diffusion - controlled. At high pressures >1.5 atm., the flux increases linearly with the total pressure which indicates that the transport is predominantly convection - controlled (27).

In most applications the rate limiting step in chemical transport reaction is the vapour phase diffusion processes. This is largely the result of the use of gas pressures less than the convective regime but greater than 0.01 atm. where the non-free-molecular flow gas motion is usually slow as compared with the chemical reaction rate. It therefore follows that the

transport rate is often directly proportional to the concentration gradient (from Fick's law) of the transport species and inversely dependent up on the total gas pressure (from diffusivity theory) (7).

The maximum capacity of our reactor is about 2 atm. and hence we expect that it is in the diffusive regime resulting that the transport increases with increase in the concentration of the transport agent which is iodine.

1.1.3.3 Geometry of the tube

Tube geometry has something to do in varying the transport mode. Most of the experiments attempted for different compounds witnessed that the range of the predominant convection is extended to lower pressures with increasing the diameter of the tube (8).

In some cases relatively small length-to-diameter ratios increase the growth rate (17) although in other cases the geometry of the tube does not have any appreciable effect (10). In our case the length of the tube is varied from 100 - 120 mm long with ID of 14 mm. This range of length was found to be manageable for designing the reactor. Too short a length will make the sealing off more difficult and too long a length of the reactor will cause the transport hindered since it won't get along with the furnace design.

Samarium monochalcogenides exhibit interesting peculiar characteristics. Use is made of these special properties of these compounds in the production of opto-electronic and acousto-electronic equipment (28).

So far in the literature no report was made on the chemical transport reaction of samarium monochalcogenides. The topic of our interest is to see if the transport of these compounds is possible using iodine as a transport agent.

To do this, the following steps were taken.

- Theoretical calculations for various transport systems were performed to obtain the optimum operating conditions such as T_s , T_d , and Δp .
- Preparation of SmX (X = Se, Te) was conducted
- CTR of SmX
- The crystals grown were then characterised.

2.LITERATURE REVIEW

2.1 *Rare - Earth Chalcogenides.*

Single crystals growth of LnX compounds (where Ln = Sm, Eu, Yb and Tm, and X = S, Se and Te) are hindered because of their high melting points (1500 - 2700 °C) and because of the reactivity of the lanthanide metals with container materials.

Chemical transport technique provides a distinct advantage in growing such high melting compounds because in this technique crystals can be grown at temperatures well below their melting points (30).

The rare - earth chalcogenides posses interesting magnetic, optical, and electrical properties (31 - 33). Because of lack of single crystals most magnetic, electrical ,and optical measurements have been made on powder samples (10). It is of interest therefore to prepare single crystals of these compounds since these compounds can better be understood with measurements on single crystals.

2.1.1 *Oxidation State*

The +3 state of oxidation is a characteristic of all lanthanides both in the solid and in the solutions in water and other solvents. Hence in our case chalcogenides of the form Ln₂X₃ is most likely to be formed together with the monochalcogenide. A few solid compounds exemplifying the +4 state have been prepared. From the lanthanide groups Ce, Pr and Tb exhibit +4 oxidation state. Solid compounds separated in a state of purity with +2 oxidation state is limited to groups of lanthanides such as Eu, Yb, Sm and Tm.

Therefore, in the preparation of samarium monochalcogenides SmX ; Sm_2X_3 and the intermediate compound between the two, Sm_3Se_4 is expected to be formed in various amounts depending on the technique adopted (34).

2.1.2 Crystallographic structures

At normal conditions, bulk forms of all rare-earth monoselenides have a cubic NaCl structure, space group $\text{Fm}\bar{3}\text{m} - \text{O}_h^5$ (No. 225) ; $Z = 4$, Landelli *et al.* (35). A pressure induced valence transition is observed for SmSe retaining the cubic NaCl structure. The formula Sm_3Se_4 and the sesquiselenide form both exhibit the cubic unit cell with space group $\text{T}43\text{d} - \text{T}_d^6$ (No. 220).

Samarium telluride has cubic NaCl structure with space group $\text{Fm}\bar{3}\text{m} - \text{O}_h^5$ (No.225); $Z = 4$, Landelli *et al.* (36). SmTe shows a phase transition from NaCl type to CsCl type structure at high pressure (8 to 11 GPa) and furthermore an iso - structural pressure induced valence transition from +2 to +3 is observed. The sesquitelluride form exhibits the orthorhombic U_2S_3 type, space group $\text{Pbnm} - \text{D}_{2h}^{16}$ (No. 62) ; $Z = 4$.

In our condition, both compounds are prepared at relatively very low pressure hence such valence transitions due to pressure are precluded.

2.2 Formation of Rare - Earth Monoselenides

2.2.1 Preparation of Polycrystals

The most common preparation method for MSe is that from the elements. This is performed in a two step process; In the first step, small metal chips are reacted with a calculated amount of selenium in a sealed ampoule at 760 Torr H_2 by slowly heating to

600 ° C and holding the temperature for a few hours. In the second step, the product obtained is briquetted at 8 to 10 K bar in dry CO₂ or Ar. It is then inductively annealed at 1600 ° C to 1800 ° C in a continuous vacuum of ca. 5*10⁻⁵ Torr in a Mo or Ta crucibles for 1 to 2 h, Glubkov *et al.* (37). This method yields macrocrystalline specimens. In this method direct contact between the components, which would give a violent reaction, is prevented by placing the selenium in a tube.

First step reaction in direct contact in evacuated quartz ampoules and prolonged final heating at relatively low temperatures in Ar or vacuum often gives inhomogeneous samples. Reaction temperature reported for the first step are, for example, 400 °C (M = La to Nd), Landelli (35), 600 °C (M = Y, Gd to Yb), Landelli (35), 800 °C (M = La to Nd, Sm), Nagai *et al.* (34). Examples for the final heating are: 1000 to 1100 °C (M = La to Nd, Sm), 1100 to 1400 °C (GdSe), Landelli (35), 2 h at 1300 °C in Pythagoras crucibles (DySe) Olcese (35), 2 h at 1400 °C, (HoSe), Bruzzone (35), 1350 °C (ErSe), Bruzzone (35).

Samarium monoselenide can be prepared from Sm₂Se₃ at 1700 °C in vacuum, Guitard, Benecerrrat (35). Thermal decomposition of the sesqui - selenides M₂Se₃, M = La to Nd, or the diselenides at 1800 °C and 10⁻⁴ Torr results in a mixture of MSe and M₃Se₄, Obolonchic, Mikhilan (38).

Monoselenide samples which differ slightly from stoichiometric composition can be prepared by the so - called metallo - hydride method as :



with X = 2 for M = La, Ce, Pr, Nd, Sm, Obolonchic, Mikhlian (38), Ho, and Er ; X = 0.8 for M = Sc, X = 1.4 for M = Tm, and X = 1.8 for M = Yb, Skripka *et al* (35).

Samarium selenide is prepared by reaction of samarium turnings and selenium in supramax glass tubes sealed at 10^{-3} to 10^{-4} Torr for nearly 14 h at 500 °C. The pressed reaction product, still heterogeneous, is then heated at 500 °C in tantalum vessels in an Ar atmosphere enclosed in a sealed quartz tubes. Completion of the reaction is reached after 14h at 1100 °C. A sample with a formal composition of $\text{SmSe}_{1.1}$ contains Sm_3Se_4 as a by product, Landelli, Palenzona (35).

Samarium selenide can also be prepared by heating a mixture of elements in a vacuum sealed quartz tube slowly to 1000 to 1050 °C and this temperature is then held for 10 to 15 h, Landelli (39).

2.2.2 Formation of Single- Crystals

a. Growth from the melt

Growth of single crystals from the melt is performed in Ar, Golubkov *et al.* and Batlogg *et al.* (36,41). Ingots, which contain large single crystal sections of MSe, M = Ce, Nd, Sm, Gd, and Yb were obtained in Ar by slowly cooling inductively heated melts contained in upright Ta crucibles. Typical cooling rates down to 1000 °C were 20 K/min, Miller *et al.* (35).

b. Growth by sublimation

Single crystals of MSe, M = Nd, Sm, Eu, Gd, and Yb may be grown by sublimation in a sealed W or Mo crucibles, which are hung by tungsten wires in vertical furnaces heated either with high frequency induction or resistivity, Kaldis (42).

Mechanically perfect single crystals of SmSe, EuSe, and YbSe, 1 cm or more in length, were prepared by inductively heating a powdered mixture of rare earth metal and MSe (< 75 mol %) in a W, Re, or Mo crucibles which was degassed and then sealed.

c. Growth by CTR

Crystal growth by a chemical transport reaction is done in Mo crucibles. The transporting agent for YbSe was I_2 (38) and for EuSe was I_2 and EuI_2 . Mass spectroscopically pure EuSe crystals are obtained at >1850 °C.

2.3 Formation of Rare-earth Monotellurides

2.3.1 Formation of Polycrystal

The rare earth monotellurides MTe were prepared like the other tellurides (M_2Te_3) by reacting appropriate quantities of Te and M in the form of chips in a sealed evacuated tube at about 600 °C for 18 to 24 h, followed by further reaction near 900 °C for 3 to 4 h and repeatedly melting the thoroughly homogenised material in a sealed Ta tube, Jayaraman (43).

For the reaction in evacuated ampoules the temperature was held for 2 to 3d at 400 to 450 °C. After cooling, the brown powders are pressed under CO_2 followed by annealing in quartz ampoules. Me_3Te_4 , formed intermediately via M_2Te_3 , transforms at 1100 °C slowly to MTe, Landelli (36).

2.3.2 Preparation of Single Crystal

a. Growth by sublimation

Single crystals of MTe (M = Nd, Sm, Eu, Gd, Ho, Er, Yb) were grown by high temperature vapour growth in sealed Mo (or W) crucibles, for example, at a temperature gradient of 1960 → 1950 °C and a growth rate of approximately 12.5 mg/h. The chemical transport takes place via the formation of M - Mo complexes. Iodine was used as a transporting agent for YbTe, and iodine, EuI₂ or EuBr₂ were used in the case of EuTe, Kaldis (42).

b. Growth by CTR

The chemical transport reaction with iodine as a carrier gas was used by Khan et al (44) to prepare MTe with M = Tb, Dy, Er, Dy, Er (45), Tm, Lu (45) or to prepare mixed crystals (M M') = (Dy, Tb), (Dy, Er), (Er, Tb), or (Lu, Tm) (45). The transport took place, for example, at a temperature gradient Δt between 25 and 75 °C with in the range 1000 to 950 °C in ampoule of ca. 25 ml volume and an iodine concentration of (5 to 6.5) mg/ml or 7 to 9.3 mg/ml. Element mixtures of 0.5 g to 1 g were transported within 72 h (43 - 45).

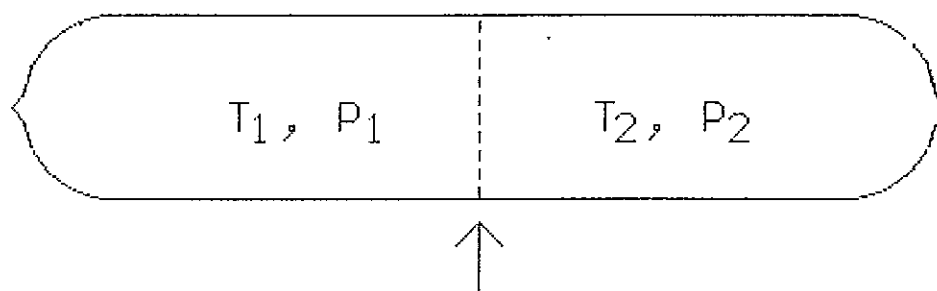
3. THERMODYNAMICS

3.1 Thermochemical calculations

Thermodynamics in general gives information about the equilibrium reactions of substances. What makes us more interested is how one can arrive at the kinetic information (transport rates) of such reactions using thermodynamics.

For this we have adopted the frequently applied model (46). This approximate model can be constructed on the following assumptions:

- 1- The ampoule is divided into two equal parts as shown in the fig. below.



Ideal Boundary

$$\Delta P = P_2 - P_1$$

Fig.2 A model showing the ideal division of the ampoule.

- 2- Half of the tube is at T_1 and half at T_2 .
- 3- The solid phase at T_1 and T_2 is in complete equilibrium with the vapour. This means that kinetic barriers at the vapour-solid interfaces are assumed to be negligible.

The change in the partial pressure of the transporting species, for instance SmI_2 in our case, is the one that plays the vital role in the rate of transport. Of course, the rate increases linearly with the difference in partial pressure (ΔP) of SmI_2 in both parts of the ampoule.

To calculate the optimal T_1 , T_2 , and the amount of halogens that is to be introduced into the reactor the following steps are carried out.

1- Thermodynamic data for the substances of interest are collected as shown in the table below.

Table 1 Some thermodynamic data used in the computations concerning the reactions given in section 3.3.

Subs.	State	$\Delta_f H_{298}^0$ (KJ/Mol)	ΔS_{298}^0 (J/Mol K)	$C_p = a + bT + cT^{-2}$			Temp. Interval	Ref.
				a	b*10 ⁺³	c*10 ⁻⁵		
SmS	(S)	-431.79	101.04	52.20	-	-	-	47,48
SmSe	(S)	-368.82	89.86	50.21	-	-	-	35,49,53
SmTe	(S)	-309.61	97.09	51.88	-	-	-	36,52,53
SmBr ₂	(g)	-410.03	20.52	91.46	-	-	298 - 1000	50
SmI ₂	(g)	-292.88	353.30	66.40	-	-	298 - 1000	51
S ₂	(g)	127.52	228.03	36.48	0.67	-3.76	298 - 3000	54 -57
Se ₂	(g)	138.64	251.96	36.52	1.34	-1.47	-	54 -57
Te ₂	(g)	171.54	168.57	37.02	0.67	-2.84	-	54 - 57
Br ₂	(g)	30.80	245.37	37.32	0.50	-1.26	-	54 -57
I ₂	(g)	62.44	260.60	37.40	0.58	-0.71	459 - 3000	54 -57

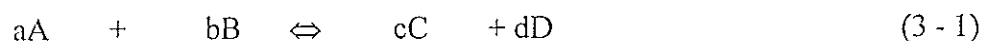
2- By making use of these data the change in the free energy of the reaction ΔG_R is calculated. .

Of particular interest to us in considering a chemical reaction is the standard free energy of the process. It should be emphasized at this point that the sign of ΔG^0 for a particular reaction can be used only as a criterion of spontaneity if all substances are in their

standard states. The real significance of ΔG° lies not in connection with the predictability of spontaneity but in connection with equilibrium constants.

To come up at such relationships from available thermodynamic data one needs to use the following fundamental laws of thermodynamics.

The first is simply the law of conservation of energy. One important corollary is Hesse's law (58-60), which states that the total energy changes in a series of reactions depends only on the nature of the initial and final products and is independent of the number and nature of any intermediate reactions. This is the basis for the calculation of heats of reaction ΔH_R by subtracting the heats of formation ΔH_f of reactants A, B from those of the products C, D. Thus in a reaction involving stoichiometric coefficients a, b, c and d:



$$\Delta H_R = d\Delta H_f(D) + c\Delta H_f(C) - b\Delta H_f(B) - a\Delta H_f(A) \quad (3-2)$$

The second one is Kirchhoff's law (58-60): the rate of change of the heat of any reaction with temperature is equal to the difference between the heat capacities C_p of the products and those of the reactants. Thus, the change in the heat capacity of the system at constant pressure for the foregoing reaction is :

$$\Delta C_p (R) = d\Delta H_R / dT = dC_p(D) + cC_p(C) - bC_p(B) - aC_p(A) \quad (3-3)$$

Since most reactions occurred above room temperature (298.15 °K), the heat capacity is frequently expressed by an algebraic equation :

$$C_p = a + bT + cT^2 \quad (3-4)$$

accordingly :

$$\Delta C_p (R) = \Delta a + \Delta bT + \Delta c'T^2 = d\Delta H_R / dT \quad (3 - 5)$$

Upon integration between some convenient temperature T_0 , usually 298.15 °K and T:

$$\Delta H_R (T) = \Delta H_R^0 + \Delta aT + 0.5\Delta bT^2 - \Delta c'T^{-1} \quad (3 - 6)$$

From the second law of thermodynamics a new state function, entropy S, is introduced. By analogous expression that is used for enthalpy, entropy of a reaction can be calculated as follows for equation (3 - 1)

$$\Delta S_R = dS (D) + cS (C) - bS (B) - aS (A) \quad (3-7)$$

Since as described in equation (3 - 4), C_p may be expressed as an analytical function of temperature, ΔS can be readily obtained by integration of the following equation.

$$dS = C_p / T dT = C_p d\ln T \quad (3-8)$$

Thus ΔS can be given as

$$\Delta S_R (T) = \Delta S_R^0 + \Delta a\ln T + \Delta bT - 0.5\Delta c'T^{-2} \quad (3 - 9)$$

where ΔS_R^0 is the change in the entropy of a reaction at standard state.

For chemical reactions occurring at constant temperature and pressure :

$$\Delta G = \Delta H - T\Delta S \quad (3-10)$$

where ΔG is Gibbs free energy of the reversible reaction.

The change in the Gibbs free energy can also be related with equilibrium constant by the well - known equation (61):

$$\Delta G = -RT \ln K_{eq} \quad (3-11)$$

this very important equation is the basis for calculation of the equilibrium constant from thermal data. Once we have the equilibrium constant we will be able to calculate the partial pressures of the gaseous species since the equilibrium constant can be expressed as the ratio of the partial pressures of the products and the reactants.

The partial pressure differences were calculated on the assumptions of diatomic gases of selenium and tellurium respectively (62). The samarium iodide (SmI_2) partial pressure X , was then obtained from the cubic equation

$$\frac{X (0.5 X)^{1/2}}{(P^0 - X)} = K_{eq}(T) = \exp(-\Delta G / RT) \quad (3 - 12)$$

where P^0 is the partial pressure of I_2 ideal gas generated by iodine.

3.2 The Program

- It used all thermochemical data of the substances and various amount of transport agent as an input.
- It takes for T_1 and T_2 , respectively, all values between 300 - 1300 °K in distance of 2.5 °K and calculates for each pair of T_1 and T_2 the corresponding ΔP .

- It transfers the value of ΔP in a colour scale and draws the corresponding colour in a diagram with T_1 and T_2 as X - and Y- axes, respectively. The advantage of this is that one can easily select the probable ranges in relatively short time.
- It draws a light gray colour if the calculation ends in the casus irreducibilis.
- It draws a dark gray colour if any pressure goes beyond 2 atm.
- The program is written in Turbo Pascal 6.0 of Borland International, InC.

3.3 Selection of Optimum Operating Condition

We have made calculations to find the optimum operating conditions for the following tentative transport systems:

SmS with Bromine;

SmS with Iodine;

SmSe with Bromine;

SmSe with Iodine;

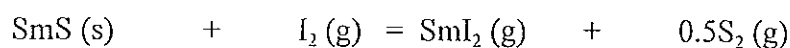
SmTe with Bromine;

SmTe with Iodine.

in all cases, the concentration of the transport agents was varied from $1 \cdot 10^{-5}$ mol / c.c. to $5 \cdot 10^{-5}$ mol / c.c.. The results obtained are discussed in the following sub-sections

3.3.1 Transport of SmS with Iodine

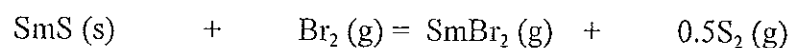
The transport reaction for this compound can be described in the following way :



For such a transport system, iodine could not serve as a transport agent since it results in relatively low ΔP ($P_s - P_d$) in any combination of T_s and T_d . This condition persists with different concentrations of the transporter. Besides, with increasing concentration of iodine the maximum temperature that limits the allowed pressure range decreases from 1300 °K to 800 °K and at concentrations of iodine with 0.00003 mol/c.c the change in the partial pressure declines to a minimum value. (see Appendix II).

3.3.2 *Transport of SmS with Bromine*

The reaction can be described as follows :

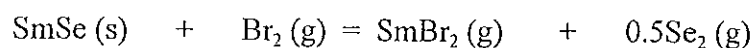


This reaction results in attaining a change in partial pressure which is greater than 0.05 atm. for every possible combinations of temperatures where the maximum temperature is below 600 °K. Compared with iodine, bromine is preferable for it is possible to get the same pressure difference by using relatively lower temperature. For instance, one can use the following temperature ranges for the source as well as deposition zones, respectively. $T_s = 450 - 600$ °K and $T_d = 300 - 350$ °K. In this case one can not use a bromine concentration greater than $3 \cdot 10^{-5}$ mol / c.c. for using this concentration can lead to a pressure of greater than 2 atm. which is perhaps above the capacity of the ampoule.

One can also observe that with increasing the concentration of bromine the range of temperature decreases making the probability of selecting the best operating condition minimum. However, this is also not chosen for the experimental part because of the difficulty in managing the fluid transport agent.

3.3.3 Transport of SmSe with Bromine

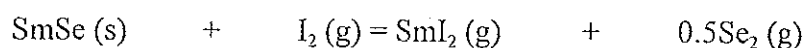
The reaction can be stated in the form:



In this regard bromine can not serve for transporting samarium selenide. To start with, for any possible combinations of temperatures for the source and deposition zones one can not see any colour representing the corresponding change in the partial pressure of the samarium bromide. This is true when the total pressure goes beyond the limit in all cases. Besides the fluidic nature of the bromine makes it difficult to use it as the transport agent.

3.3.4 Transport of SmSe with Iodine

The reaction is as depicted in the following scheme:



Samarium selenide can be transported using iodine as a transport agent at relatively lower temperatures. Different combinations can be used. For instance, $T_d = 300 - 500$ °K and $T_s = 500 - 700$ °K. Therefore, we can have different ways of combining T_s and T_d to get nearly similar value for the partial pressure differential of samarium iodide.

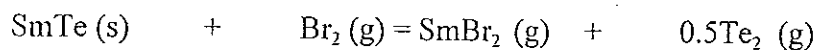
The other characteristics exhibited by this compound is that as the iodine concentration increases, the temperature range decreases. As can be seen from the graph (see Appendix 2) the maximum temperature that was nearly 700 °K for $1 \cdot 10^{-5}$ mol / c.c. of iodine

goes down to 600 °K for $2 \cdot 10^{-5}$ mol / c.c. and further decreases down to 550 °K for $3 \cdot 10^{-5}$ mol / c.c. of the transport agent iodine .For a concentration of iodine beyond $3 \cdot 10^{-5}$ mol / c.c. the program shuts off since the total pressure goes above the limit. Thus, one should be able to make a favourable compromise of both the concentration and temperature ranges for nearly the same pressure differences.

Sometimes there are cases where the value of the change in the partial pressure differences for the gaseous species samarium iodide to be relatively low while exhibiting a relatively larger value of temperature profile. Sporadically ,this could be preferable to those with the opposite from the point of view of kinetics. A case in point is that, at a temperature range between 500 - 700 °K for T_s and 300 - 500 °K for T_d a pressure difference of greater than 0.05 atm. can be obtained. If one chooses a relatively higher temperature for the source temperature, i. e. $T_s = 500 - 850$ °K keeping the deposition temperature the same, the relative change in the partial pressure will be in the range 0.01 - 0.05 atm.

3.3.5 Transport of SmTe with Bromine

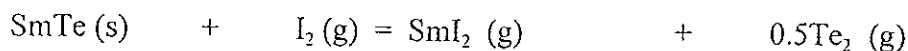
The reaction can be described as follows:



According to the result obtained, bromine could not serve as a transport agent to samarium telluride for the same reason discussed in the case of SmSe with bromine.

3.3.6 Transport of SmTe with Iodine

The reaction is as depicted below:



The thermodynamic result predicted that iodine can be used for the transport of samarium telluride. As predicted theoretically, a relatively higher change in partial pressure difference of samarium iodide can be obtained for temperatures of the source and deposition region in the range as written below.

$$T_s = 350 - 480 \text{ }^\circ\text{K},$$

$$T_d = 300 - 350 \text{ }^\circ\text{K}, \quad \text{and / or}$$

$$T_s = 700 - 1300 \text{ }^\circ\text{K},$$

$$T_d = 450 - 550 \text{ }^\circ\text{K}.$$

Similar to samarium selenide, the range of temperature decreases with increasing the concentration of the transport agent iodine. Unlike the case of samarium selenide/iodine, a different condition is observed. As the concentration goes from 1- to 2- then to 3×10^{-5} mol/c.c. then the probability of using almost all temperature values within the limit is enhanced. For instance, when the concentration of iodine is 2×10^{-5} mol/c.c. one can't use the combination $T_d = 310 \text{ }^\circ\text{K}$ and $T_s = 350 \text{ }^\circ\text{K}$ since it results in pressure difference of samarium iodide which is in the range between 0.005 - 0.01 atm. which is small as compared to > 0.05 atm. that could be obtained when one uses a concentration of iodine nearly 3×10^{-5} mol/c.c.

3.4 Conclusion of the Calculation

The compounds chosen for the experimental part are samarium selenide and samarium telluride iodine being a transport agent for both compounds. The selected optimum operating condition to conduct the experiment are

- For SmSe: $T_s = 668 \text{ }^\circ\text{K}$ and $T_d = 475 \text{ }^\circ\text{K}$
- For SmTe: $T_s = 717 \text{ }^\circ\text{K}$ and $T_d = 503 \text{ }^\circ\text{K}$.

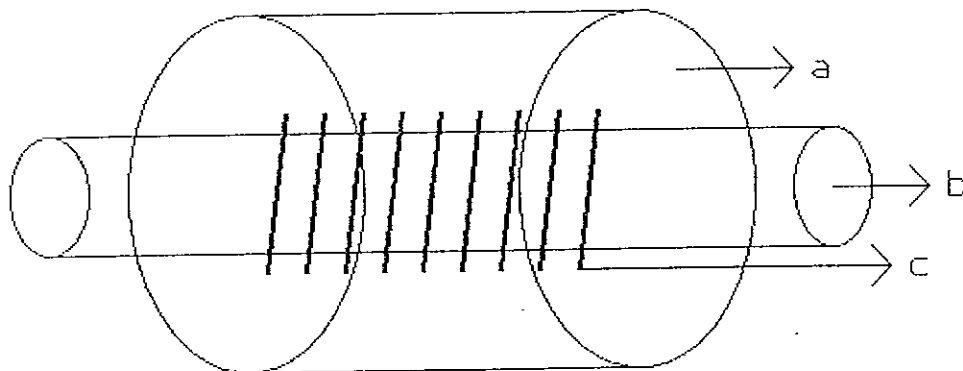
4. EXPERIMENTAL

4.1 Construction of the Transport Furnace

The main parts of the resistance furnace are the heating element, the heating element support, and the heat insulating filler. The resistance material is named by Kanthal (10) which is expected to serve up to a temperature of 1100 °C with a working media of air. This metal wire is wound on a cylindrical support which is made of some insulating material.

The tubular refractory material is 24 cm long with 3.20 cm ID and 4.42 cm OD. The wire is wound on 20 cm length of the tube with 2 cm space from each side having nearly 1-1.5 mm gap between the coiled wires.

After winding of the wire is completed, it is washed with doubly distilled water so many times and was allowed to dry at ambient temperature followed by cementing with the heat insulating filler (63).



a - metal casing

b - tubular refractory

c - Kanthal wire

Fig. 3 Tubular furnace

The heat insulating filler usually made of the same material as the tube furnace was made in to paste using deionized water and then let dried for one week by exposing to air.

At last the tubular furnace was wrapped with special ceramic fibre and placed in a metal casing which acts as a support for the fibre as shown in the Fig. 3.

The furnace was then connected to a variable transformer having different taps (0 - 100%), the number of taps indicating the corresponding voltage to be supplied to the oven. As the number of taps increases the voltage supplied will increase resulting in raising of the temperature.

The oven was regulated by a digital thermocouple of type RS -612-625 having a length of 30 cm and 3 mm OD. Since the thermoelectric power of the thermocouple may deteriorate during its use it was calibrated before use (and in fact after long use) with baths of known temperatures.

We made use of an ice and water with different temperatures where the temperatures are measured by standard thermometers. The thermocouple has two screws one for adjusting the absolute temperature and the other adjusting for the relative change in the temperature. Using these screws we calibrated the thermocouple in accordance with the reading of the thermometer.

4.2 Preparation of the quartz glass tube

The tubes used for preparation of SmSe and SmTe from the elements and for the transport experiment are made of transparent pure silica (quartz) glass. They are carefully washed with doubly distilled water before the sample is introduced. The tube is designed to the reactor by using oxygen - acetylene flame with length of 10-12 cm, ID of 14 mm, and OD of 17.7 mm.

The transport agent I_2 is solid at ambient temperature and the mode of incorporating the samples in to the reactors is as follows:

1- Selenium is weighed in solid form, with out particular care. The ampoule is sealed by a table top vacuum pump. The same holds true for tellurium.

2- Iodine which is very hygroscopic product is weighed with out any special care and added in to the transport tube (23, 66)

After the samples are introduced in to the reactor (quartz ampoule) the tube is evacuated at 10^{-3} - 10^{-2} Torr (65) and sealed off while maintaining one side of the ampoule where the samples are loaded in an ice and salt mixture. This is to prevent the samples from vaporisation during sealing.

4.3 Synthesis of the Samarium Selenide Powder

Weighed quantities of elements 0.179g (Sm) and 0.103g (Se) in the atomic ratio of 1:1 were introduced in to the previously cleaned quartz tube (64,65), 120 mm long and 14 mm ID and sealed under vacuum (65).

The ampoule was then placed in to the thermolyne furnace. During synthesis, the temperature was increased up to 600 °C in 13 h, stepwise in order to avoid all explosion risks due to rapid selenium vaporisation (12). Then the system was increased slowly up to 1000 °C to 1050 °C and kept constant. Finally the reactor is let cool down slowly to ambient temperature.

4.4 Synthesis of the telluride powder

Weighed quantities of elements 0.163g (Sm) and 0.137g (Te) in stoichiometric ratio were introduced in to the previously cleaned quartz tube (64 -65), 100 mm long and 14 mm ID and sealed under vacuum (65).

The ampoule was then placed into the muffle furnace. The temperature of the thermolyne furnace was increased in steps of 50 °C from room temperature to a temperature of 600 °C. Then the ampoule was kept at this specific temperature for 12 h. Finally the temperature was raised gradually up to 1000 °C - 1050 °C and kept within this temperature range for 11 h. The slow heating was necessary to avoid any possibility of explosion due to the exothermic reaction between the elements. At last the ampoule was allowed to cool slowly to room temperature.

4.5 Optimisation of the furnace

During crystal growth, the temperatures produced in the different areas of the tubular furnace must be well known in order to select the best area upon which the reactor is placed to get good quality of the substance to be transported.

The temperature obtained in the tubular furnace depends on the following factors.

1- Position in the furnace

The temperature distribution in the tubular furnace depends on the furnace condition. If both ends of the tube are closed or opened, then the temperature profile is symmetric with the highest temperature in the middle in both cases but the gradient is larger for the latter. If on the other hand one end is closed and the other end is open, then the temperature distribution is asymmetric with a large temperature profile. All these were attempted to

maximise the chance of selecting the required temperature distribution for the substances of interest. It is worth noting that the measurement was made at 5 cm and 6 cm intervals with various tap positions.

2 - Tap position of the transformer

As the tap position of the transformer increases (0 - 100 %) there is a linear increment on the furnace temperature.

3 - On the time the furnace is switched on

A linear increment in the temperature of the furnace is observed for a while until it reaches a steady state equilibrium. The time that is required to attain such a state was found to be about 30 minutes. Therefore, use is made of this time to change the tap position of the transformer. However, for the same tap position the time required to measure the temperature between two consequent distances was 10 minutes.

To find the best conditions in accordance with the result obtained from thermodynamic calculations the following tests were performed and the results are depicted as follows. For tap positions which are used for the experiment we presented it in the form of table but for the remaining taps we presented in the form of graph, in Appendix 3.

Table2 : Temperature distribution on the furnace

	<u>Tap Position 13%</u>				
Distance (cm)	5	10	15	20	25
Ave. Temp. (°K)	549	723	773	501	448

Tap Position 10 %

Distance (cm)	5	10	15	20	25
Ave. Temp. ($^{\circ}$ K)	478	618	668	613	380

4.6 Chemical transport of SmTe

0.1120g of SmTe and $2 \cdot 10^{-5}$ mol/c.c of iodine were introduced into the previously cleaned quartz ampoule (8) of 12 cm long and 14 mm ID. The evacuation and sealing of the ampoule was performed by the method described so far. The whole process was conducted as depicted in the Fig. 4 below.

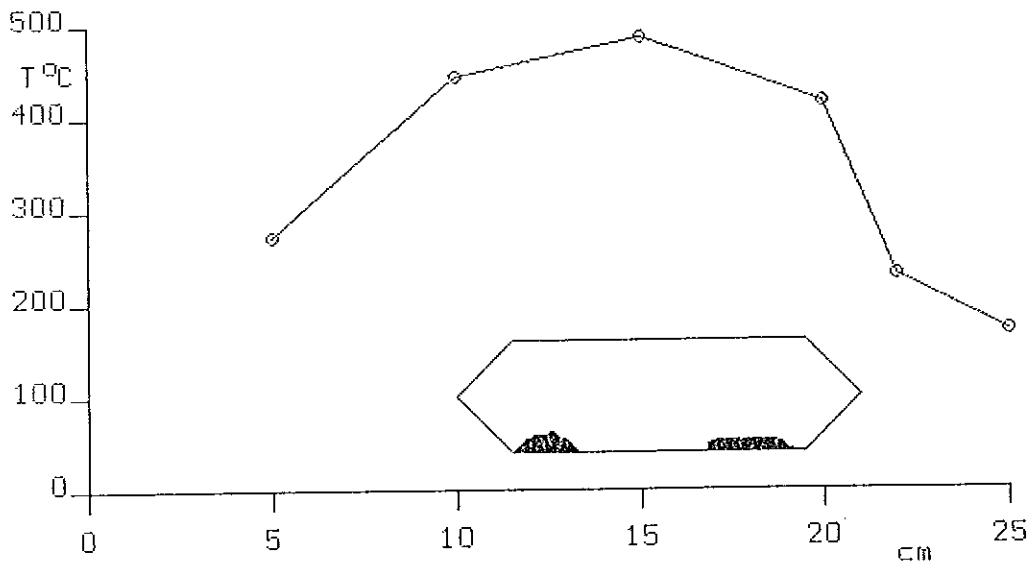


Fig. 4: Temperature distribution in the furnace. Tap position 13% and the furnace one side open.

The ampoule was placed for three days and allowed to cool in air. Then the reactor was cut open and both the transported material and the residue together with the initial raw material were analysed in Germany by X-ray analysis.

4.7 Chemical transport of SmSe

0.1000g of SmSe and $2 \cdot 10^{-5}$ mol/c.c of iodine were added into the already cleaned quartz tube of 10 cm long and 14 mm ID. The method for evacuation and sealing of the reactor was similar to that of SmTe but in this case the tube stayed in the furnace for nearly 10 days. The position of the ampoule and the temperature distribution is as shown in the Fig.5

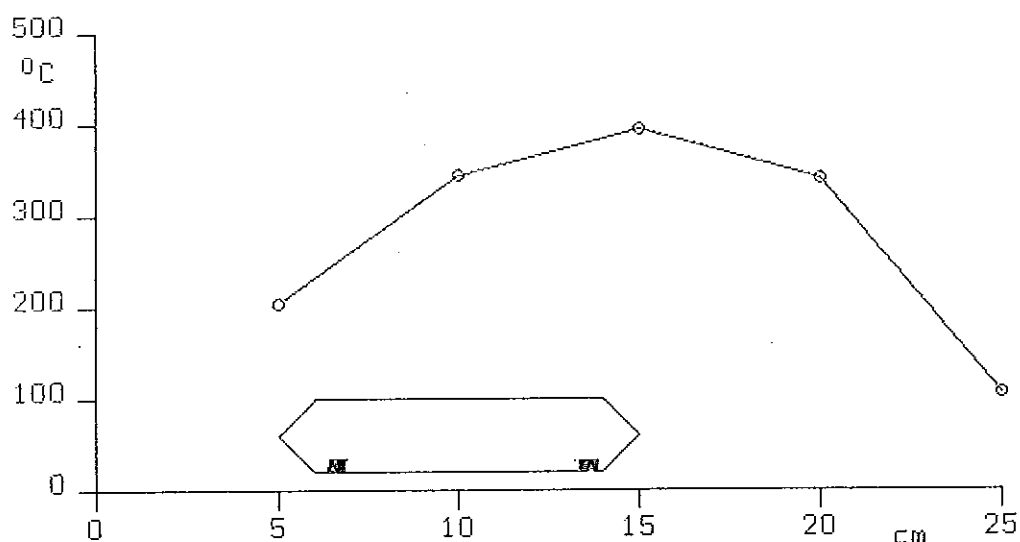


Fig. 5 Temperature distribution in the furnace. Tap position 10% and the furnace one side open

5. Characterisation of products by X- ray Powder Diffraction Technique

5.1 Principles and Uses of Powder Diffraction Method

The X-ray powder diffraction technique can be conveniently used for identification and characterisation of solids, especially inorganic solids.

Each crystalline phase has a characteristic powder pattern which can be used as a finger print for identification purpose (68). The two variables used in the powder pattern are peak position i.e. d- spacing which can be measured very accurately if necessary, and intensity which can be measured either qualitatively or quantitatively. The normal practice in using powder patterns for identification purposes is to pay most attention to the d-spacings but at the same time .check that intensities are roughly correct (69).

Some of the advantages of this technique are the following :

- different substances can be identified together for there is no interaction between the patterns of the different phases.
- the intensity of the patterns of one phase differs from the others depending up on the concentration of the substance in the sample.

There are two factors which determine powder patterns :

- a. the size and shape of the unit cell i.e. lattice constant and
- b. the atomic number and position of the various atoms in the cell i.e. the crystal structure

Therefore, two materials may have the same crystal structure but almost certainly they will have quite distinct powder patterns. For instance, SmSe and SmTe both have the rock salt structure and should show the same set of lines in their powder patterns, but the positions and intensities of the lines are different in each. The positions or d-spacings of the lines are shifted because the unit cells are of different size and therefore, the a parameter in the d

-spacing formula varies. Intensities are different because different anions with different atomic numbers and therefore with different scattering powers are present in the two materials, albeit the atomic co-ordinates are the same for both (i.e. cations at corner and face centre position, etc.).

If the substance's space group, point group, and other necessary parameters are known, then it is possible to calculate the intensities of all lines by using a commercially available computer program (70, 73 -74). This is important to identify the remaining lines.

5.2 Measurement of Powder Diffraction Pattern

The equation applied is the Bragg's law.

$$2 d_{hkl} \sin\theta_{hkl} = n\lambda \quad (5-1)$$

where n is the order of reflection and can be taken as unity, λ is the wavelength of the incident X-radiation, d_{hkl} is the distance between adjacent (hkl) planes, hkl are the Miller indices and θ_{hkl} is the glancing angle corresponding to the respective Miller indices (hkl) .

To obtain d -spacings from the film the following steps are used.

1. The distances D_1, D_2, \dots of the lines are measured in mm.
2. The Bragg angle θ_{hkl} can be obtained from the relation.

$$\theta_{hkl} = D/4 \quad (5-2)$$

where the factor 4 is specific for the equipment used.

3. Then $d_{hkl} = n\lambda / 2 \sin\theta_{hkl}$

In the equation described in step 3, λ is known for $\text{CuK}\alpha_1$ which is 1.54051\AA . Since the objective is simply to confirm the formation of a material as a result of transport, a comparison of the observed d_{hkl} values is made with the reported literature data. For the identification of the unknown crystalline materials we used an invaluable reference source i.e. the powder diffraction file. In the search indices, materials are classified either according to their most intense peaks or according to the first eight lines in the powder pattern in order of decreasing d-spacings.

5.3 Characterisation of Products by Guinier Powder Diffraction

In both cases the polycrystalline form, the residual material and the transported product were analysed. The X-ray (2 θ , 71 - 72) measurements employed a Guinier-Camera ($\lambda \text{ CuK}\alpha_1 = 1.54051 \text{ \AA}$) and a silicon internal standard ($a_0 = 5.43070 \text{ \AA}$). The Miller indices, the d-spaces, and intensities calculated by a computer program for SmSe and SmTe are listed together with corresponding lines in the sample as shown in the following tables.

Table4 X-ray data for SmSe raw material

Line No.	I/I_0	hkl	d (meas.)	d (calc.)
1	170	111	3.5763	3.5782
2	1000	200	3.1064	3.0990
3	737	220	2.2033	2.1933
4	265	222	1.7946	1.7892
5	128	400	1.5526	1.5495
6	88	311	1.8587	1.8687

Table 5: X-ray data for SmSe residue

Line No.	I/I_0	hkl	d. (meas.)	d. (calc.)
1	170	111	3.5888	3.5782
2	1000	200	3.0700	3.0990
3	737	220	2.2080	2.1933
4	265	222	1.7912	1.7892
5	128	400	1.5424	1.5495
6	88	311	1.8517	1.8687

Table 6 : X-ray data for SmSe transport

Line No.	I/I_0	hkl	d. (meas.)	d. (calc.)
1	170	111	3.3940	3.5782
2	1000	200	3.0634	3.0990
3	737	220	2.0765	2.1133
4	265	222	1.7700	1.7892
5	128	400	1.5230	1.5495
6	88	311	1.84990	1.8687

Table 7: X-ray data for SmTe raw - material

Line No	I/I_0	hkl	d. (meas.)	d. (calc.)
1	11	111	3.8008	3.8117
2	1000	200	3.2660	3.3010
3	752	220	2.3490	2.3341
4	7	311	1.9964	1.9906
5	273	222	1.9033	1.9058
6	132	400	1.6495	1.6505

Table 8: X-ray data for SmTe residue

Line No.	I/I_0	hkl	d. (meas.)	d.(calc.)
1	11	111	-	3.8117
2	1000	200	3.2786	3.3010
3	752	220	2.3377	2.3341
4	7	311	1.9753	1.9906
5	273	222	1.8995	1.9058
6	132	400	-	1.6505

Table 9: X-ray data for SmTe transport

Line No.	I/I_0	hkl	d. (meas.)	d. (calc.)
1	11	111	-	3.8117
2	1000	200	3.3075	3.3010
3	752	220	2.3220	2.3341
4	7	311	-	1.9906
5	273	222	1.9016	1.9058
6	132	400	1.6712	1.6505

In both cases the most intense lines correspond with the calculated values of SmSe and SmTe respectively. Infact there are lines remained which are less intense, and this indicates that there are traces of other crystalline phases in addition to the samples.

The same method is also implemented to search for an interpretation of the remaining lines and in the case of SmSe two compounds were identified (70). The d-spacings and their relative intensities appear in the following tables.

Table 10: X-ray data for Sm₂O₂Se / SmSe raw material

Line No.	I/I ₀	hkl	d. (meas.)	d. (calc.)
1	113	002	3.4613	3.4550
2	1076	011	3.0554	3.0407
3	432	102	2.4268	2.4183
4	110	003	2.3076	2.3033
5	361	110	1.9650	1.9550
6	178	013	1.9092	1.9045
7	179	201	1.6520	1.6444
8	102	014	1.5418	1.5388
9	108	022	1.5276	1.5203
10	170	113	1.4946	1.4905
11	174	121	1.2650	1.2584
12	121	212	1.2041	1.2002

Table 11 :X-ray data for Sm₂O₂Se / SmSe residue

Line No.	I/I ₀	hkl	d.(meas.)	d. (calc.)
1	113	002	3.4671	3.4550
2	1076	011	3.0530	3.0407
3	432	102	2.4244	2.4183
4	110	003	2.3096	2.3033
5	361	110	1.9546	1.9550
6	178	013	1.9054	1.9045
7	179	201	1.6505	1.6444
8	102	014	1.5422	1.5388
9	108	022	1.5286	1.5203
10	170	113	1.4948	1.4905
11	174	121	1.2599	1.2584
12	121	212	1.2040	1.2002

Table 12: X-ray data for Sm₂O₂Se / SmSe transport

Line No.	I/I ₀	hkl	d. (meas.)	d. (calc.)
1	113	002	3.3940	3.4550
2	1076	011	3.0544	3.0407
3	432	102	2.4263	2.4183
4	110	003	2.3075	2.3033
5	361	110	1.9544	1.9550
6	178	013	1.8500	1.9045
7	179	201	1.6516	1.6444
8	102	014	1.5262	1.5388
9	108	022	-	1.5203
10	170	113	1.4946	1.4905
11	174	121	1.2659	1.2584
12	121	212	-	1.2002

Table13: X-ray data for Sm₃Se₄ / SmSe raw-material

Line No.	I/I ₀	hkl	d. (meas.)	d. (calc.)
1	1417	211-	3.5700	3.6089
2	1000	310	2.8014	2.7955
3	724	321-	-	2.3626
4	181	400	2.2049	2.2100
5	152	332	1.8879	1.8847
6	110	422-	1.8181	1.8050
7	141	431-	1.7303	1.7337
8	145	532-	-	1.4340
9	118	552-	1.2045	1.2030

Table 14: X-ray data for Sm₃Se₄ / SmSe residue

Line No.	I/I ₀	hkl	d. (meas.)	d. (calc.)
1	1417	211-	3.4817	3.6089
2	1000	310	2.7976	2.7955
3	724	321-	-	2.3626
4	181	400	-	2.2100
5	152	332	-	1.8847
6	110	422-	-	1.8045
7	141	431-	1.7321	1.7337
8	145	532-	-	1.4340
9	118	552-	1.2040	1.2030

Table 15: X-ray data for Sm₃Se₄ / SmSe transport

Line No.	I/I ₀	hkl	d. (meas.)	d. (calc.)
1	1417	211-	-	3.6089
2	1000	310	-	2.7955
3	724	321-	-	2.3626
4	181	400	-	2.2100
5	152	332	-	1.8847
6	110	422-	-	1.8045
7	141	431-	-	1.7337
8	145	532-	-	1.4349
9	118	552-	-	1.2030

From the above three the inference that can be made is that the compound was formed in the polycrystalline form and showed it-self with the residue one. But, in the transported material it is found to be none. This ascribes for the separation of SmSe in the transported case.

6. RESULTS and DISCUSSIONS

Thermodynamic calculations predict optimum operating conditions for both compounds. In considering SmTe one can generally get the following two options in selecting the ranges of the source and the deposition zone temperatures with various concentrations of the transport agent.

Option 1

$$T_s = 350 - 580 \text{ }^\circ\text{K}$$

$$T_d = 300 - 350 \text{ }^\circ\text{K}$$

Option 2

$$T_s = 700 - 1300 \text{ }^\circ\text{K}$$

$$T_d = 450 - 550 \text{ }^\circ\text{K}$$

To make the choice one should be able to consider the furnace capacity. The furnace that was built for running the experiment exhibits the dimensions and heating capacities as described in the experimental part (see sec. 4). As observed in the appendix 3 the maximum temperature of the furnace is around 1000 °K which could be obtained when one uses the tap position above 20%. The problem encountered in using such a tap position is that the temperature gradient in the furnace diminishes making it almost uniform throughout. The length of the tubular refractory, the length of the reactor, nature and patent of the coiled resistor have impact in getting the desired temperature gradient. Our furnace is so short that it is not possible to attain the required temperature profile by using higher taps. This compelled us to seek for other parameters such as concentration.

One of the peculiar characteristics exhibited by this compound is that in using 2×10^{-5} mol/c.c of the transporter concentration for option 2, the maximum temperature that was 1300 °K decreases down to 800 °K. Certainly the temperature decreases with increasing concentration. Hence the choice is made by taking into account of the fact that the maximum capacity of the furnace is considered and besides the concentration of the transport agent is taken into consideration.

By making use of the concentration of iodine to be 2×10^{-5} mol/c.c therefore, the following advantages were registered.

- the maximum temperature of the furnace in the source zone is reduced down to 800 °K which is within the capacity of the furnace,
- the required temperature gradient is obtained, and
- relatively higher concentration results in higher transport rates.

Thus, in view of the above facts the choice is made for option 2 with concentration of iodine to be 2×10^{-5} mol/c.c. This option is also advantageous since it exhibits relatively higher source temperature and this results in higher transport rates from kinetic point of view.

In the case of SmSe, the option as for the choice of the temperature ranges is only one but we also used the same concentration of iodine. The temperature ranges for both zones are :

$$T_s = 500 - 700 \text{ } ^\circ\text{K}$$

$$T_d = 300 - 500 \text{ } ^\circ\text{K}$$

Although hints can be drawn from thermodynamic calculations so as to save time and raw materials, usually it is advantageous to perform the experiment in different cases. For instance, in selecting the optimum operating conditions for CdTe fifteen growth runs were

made and for transition metal dichalcogenides such as MoS₂, MoSe₂, WSe₂, and TaSe₂ about eighty experiments were attempted (26, 74).

Both the selenide and telluride of samarium were found to transport from "hot" to "cold" zone using iodine as a transport agent. The concentration of iodine, the source and deposition temperatures as well as the temperature gradients are depicted in the table below.

Table 16 : Optimum Operating Conditions for both SmSe and SmTe

Compound	T _s (°K)	T _d (°K)	ΔT (°K)	Conc. in mol/c.c
SmSe	668	475	193	0.00002
SmTe	717	503	214	0.00002

For both compounds the X-ray analysis data of the transported crystals was close to the theoretical value reported on the literature.

Table 17 : X-ray data for SmSe

Line No.	I/I ₀	hkl	raw-form d (meas.)	transported d (meas.)	d (calc)
1	170	111	3.5763	3.4940	3.5782
2	1000	200	3.1064	3.0634	3.0990
3	737	220	2.2033	2.0765	2.1933
4	265	222	1.7946	1.7700	1.7892
5	128	400	1.5526	1.5230	1.5495
6	88	311	1.8587	1.8499	1.8687

Table 18 : X-ray data for SmTe

Line No	I/I ₀	hkl	raw-form d (meas.)	transported d (meas.)	d (calc)
1	11	111	3.8008	-	3.8117
2	1000	200	3.2660	3.3075	3.3010
3	752	220	2.3490	2.3220	2.3341
4	7	311	1.9964	-	1.9906
5	273	222	1.9033	1.9016	1.9058
6	132	400	1.6495	1.6712	1.6505

However, in comparing the observed and theoretically calculated d-values there are some deviations. The main reason for such a variation is that the lattice constants for the same compound are not exactly the same as shown below and hence the average of these a_0 values were taken in the calculation. The purity of the material also contributes to some extent for this deviation and besides nonaccuracy in the measurement of the actual distances between the respective lines on the film can also add some deviation from the theoretically calculated d-values.

Lattice Constants of SmSe in A°

6.200 (35), 6.171 (75), 6.200 \pm 2 (76)

Lattice Constants of SmTe in A°

6.594 (77), 6.595 (36), 6.60 (36), 6.58 (77)

Growth generally occurred over the final 5 cm of the reactor. The amount of transported substance to the crystallisation zone ranges from 1 to 5% by weight of the original material, the amount of samarium selenide being higher than the samarium telluride. This is attributed to the longer period of time for SmSe stayed in the furnace as compared to the latter. It was 10 days for SmSe and 3 days for SmTe. The transported rate as observed in the experiment showed that it was higher for SmTe than SmSe despite its minimum stay in the muffle furnace. As compared to most compounds grown in this technique both compounds stayed in the furnace for relatively shorter time. For comparison the following compounds and their respective growing time are depicted in the table below.

Table 19 :Growth time of some compounds.

Compound	ZrSe ₂	TiSe ₂	HfSe ₂	ZnSe	YbAs	UO ₂	ReO ₃	NbO	HfS ₂
Growth Time in days	21	15	42	30-180	10	12	30	8-13	28
Reference No.	78	78	78	79	10	19	70	80	78

In considering the transport of SmSe two compounds have shown themselves as impurities on the film although one of them separates itself from the desired product. These two compounds are Sm₂O₂Se and Sm₃Se₄. The former co-precipitates with the substance of interest while the latter remains with the original raw material. But the amount in both cases is very much less than the desired product since the lines are weak. The d-values and their relative intensities are depicted in the following tables.

Table 20 :X-ray data for Sm₃Se₄

Line No.	I/I ₀	hkl	raw-form d (meas)	transported d (meas.)	d (calc.)
1	1417	211	3.5700	-	3.6089
2	1000	310	2.8014	-	2.7955
3	724	321	-	-	2.3626
4	181	400	2.2049	-	2.2100
5	152	332	1.8879	-	1.8847
6	110	422	1.8181	-	1.8050
7	141	431	1.7303	-	1.7337
8	145	532	-	-	1.4340
9	118	552	1.2045	-	1.203

Table 21 : X-ray data for $\text{Sm}_2\text{O}_2\text{Se}$

Line No.	I/I ₀	hkl	raw-form	transported	d (calc.)
			d (meas.)	d (meas.)	
1	113	002	3.4613	3.3940	3.4550
2	1076	011	3.0554	3.0544	3.0407
3	432	102	2.4268	2.4263	2.4183
4	110	003	2.3076	2.3075	2.3033
5	361	110	1.9650	1.9544	1.9550
6	178	013	1.9092	1.8500	1.9045
7	179	201	1.6520	1.6516	1.6444
8	102	014	1.5418	1.5262	1.5388
9	108	022	1.5276	-	1.4203
10	170	113	1.4946	1.4946	1.4905
11	174	121	1.2650	1.2659	1.2584
12	121	212	1.2041	-	1.2002

Sm_3Se_4 is most likely to appear for such a possibility of formation is anticipated because of the fact that this compound is the next stoichiometric compound beside SmSe in Sm - Se - phase diagram (81). For some reason if the Sm to Se ratio is not exactly 1:1 then one should expect traces of this compound in the product. The case for $\text{Sm}_2\text{O}_2\text{Se}$ is unavoidable even with careful treatment. Always there are some traces of H_2O and O_2 coming from the oxy-acetylene flame that is used for sealing.

But from the co-precipitation of $\text{Sm}_2\text{O}_2\text{Se}$ the inference that can be made is that by thoroughly studying the optimum operating conditions we can devise a mechanism to get this compound in better quality by deliberately adding water in the samples. Water besides supplying oxygen can also serve as a transport agent (82) but the amount should be well known since it is also the cause for most of the transported substances to cling on the wall of the ampoule(17).

To get more pure product and high transport with reasonably short time the following conditions must be fulfilled. To start with the raw materials have to be sufficiently pure to avoid the formation of impurities (17). The furnace has also be built in a better way.

In most experiments the furnace is designed in such a way that it contains two zones (79) even though in rare cases it has three zones (30) made of independently. The temperature of each zone could be controlled and stabilised separately. Chromel-alumel thermocouples placed in the two zones are used to control the temperature gradient between the two zones, and the temperature fluctuation (82) is controlled by eurotherms with in $\pm 1-2$ °C (78). The temperature gradient between the two zones therefore is kept linear. This enabled the temperatures and the temperature profile between the two zones to be controlled strictly. When we come to our furnace the gradient created in a different way since the resistor is one. Although it is possible to measure the temperatures at the different positions of the furnace it is not possible to carefully control the fluctuations within the stated range. It is known that temperature oscillations contribute quite a lot in decreasing the quality as well as quantity of crystals grown (82 - 83) therefore our product could not be as pure as the one which is obtained by using a controlled equipments. Therefore, we presume that our product would be more pure than the actual if these conditions were satisfied.

We have refrained from studying the transport phenomenon for the systems SmS / I₂ due to the limited furnace capacity (≤ 1000 °K) .However, thermodynamic calculation shows best transport for the following systems in decreasing sequence.

i - For SmS, Br₂, I₂ ;

ii - For SmSe, I₂, Br₂ ;

iii - For SmTe, I₂, Br₂.

7. CONCLUSIONS

- Chemical transport of SmSe and SmTe with iodine as a transport agent is possible.
- Thermodynamic calculations provide useful information with respect to
 - 1 selection of an appropriate chemical transport reactions for the synthesis of the material to be deposited,
 - 2 maximum achievable transport rates (maximum yield of the chemical),
- From thermodynamic results and as positively supported by the experiment the possible operating conditions for the systems SmSe / I₂ and SmTe / I₂ are T_s = 668 °K, T_d = 475 °K and T_s = 717 °K, T_d = 503 °K, respectively.
- Separation of the substance SmSe from Sm₃Se₄ is possible.
- Experimental result is in agreement with theoretical predictions.

8. REFERENCES

1. Pogge, H.P.; Kemlage, B.M.; Broadie, R.W.; *J. Crystal Growth* 1977, 37, 13-22.
2. Bhaff, V.B.; Trivedi, S.B. *J. Crystal Growth* 1977, 37, 23-28.
- 3 Kaneko, T.; *J. Crystal Growth* 1993, 128, 354 - 357.
4. Pamplin, B.R.; *Crystal Growth*, Pergamon Press Ltd.: 1st Edition, 1975 .
5. Powel, C.F.; Oxley, J.H.; Blocher, J.M.; *Vapour Deposition*, New York; 1966 .
6. Hastei, J.H.; *High Temperature Vapours (Science and Technology)*, Academic Press: New York; 1975 .
7. Schäfer, H.; *Chemical Transport Reactions*, Academic Press: New York; 1964 .
8. Weidemeier, H.; Sigai, A.G. ;*J. Crystal Growth* 1969, 6, 67 - 71.
9. Faktor, M.M.; Garret, I.; *Growth of Crystals from the Vapour*, Chapman and Hall Ltd.: London; 1974 .
10. Khan, A.; Castro, J.; Vallenilla, C.; *J. Crystal Growth*, 1974, 23, 221 - 227.
11. Weidemier, H.; Irene, E.A.; Chaudhuri, A.K.; *J. Crystal Growth*, 1972, 13 / 14
393 - 396.
12. Ujjiie, U.J.; Kotera, Y.; *J. Crystal Growth*, 1971, 10, 320 - 322.
13. Piekarczyk, W.; Gazda, S.; Niemisky ,T.; *J. Crystal Growth*, 1972, 15,
272 - 276.
14. Rimmington, H.B.P.; Balchin, A.A.; *J. Crystal Growth*, 1972 , 51 - 56.
15. Chu, T.L.; Jackson, M.; Smeltzer, R.K.; *J. Crystal Growth*, 1972, 16, 254 - 258.
16. Short, N.R.; Henry, W.G.; *J. Crystal Growth*, 1973, 20, 57 - 62.
17. Mercier, J.; Lakkis, S. *J. Crystal Growth*, 1973, 20, 195 - 201 .
18. Emmenegger, F.; Peterman, A., *J. Crystal Growth*, 1968, 2, 33 - 39.

19. Niato, K.; Kamegashira, N.; Nomura, Y.; *J. Crystal Growth*, 1971, 8, 219 - 220
20. Butler, S.R.; Bouchard, R.J.; *J. Crystal Growth*, 1971, 10, 163 - 169.
21. Shiloh, M.; Gutman, J.; *J. Crystal Growth*, 1971, 11, 105 - 109.
22. Barraclough, K.G.; Mayer, A.; *J. Crystal Growth*, 1972, 16, 265 - 270.
23. Legma, J.B.; Vacquier, V.; Casalot, A.; *J. Crystal Growth*, 1993, 130, 253 - 258.
24. Richardson, M.W.; *J. Crystal Growth*, 1974, 21, 12 -16.
25. Nolang, B.I.; Richardson, M.W.; *J. Crystal Growth*, 1976, 34, 198 - 204.
26. Al -Hilli, A.A.; Evans, B.L.; *J. Crystal Growth*, 1972, 15, 93- 101.
27. Dangel, P.N.; Wuensch, B.J.; *J. Crystal Growth*, 1973, 19, 1 - 4.
28. Dutta, A.K.; *Appl. Phys. Lett.*, 1996, 68, 1189 - 1191.
29. Kaldis, E.; *J. Crystal Growth*, 1968, 3 / 4, 146.
30. Bouchard, R.J.; *J. Crystal Growth*, 1968, 2, 40 -44.
31. Jayaraman, A.; Narayanamurti, V.; Bucher, E.; Maines, G.; *Phys. Rev. Lett.*, 1970, 25, 1430.
32. Sclar, N.; *J. Appl. Phys.*, 1962, 33, 2999.
33. Busch G.; Vogt, O.; Huuliger, F.; *Phys. Rev. Lett.*, 1965, 15, 301.
34. Trotman - Dickenson, A.F.; *Comprehensive Inorganic Chemistry*, Pergamon Press Ltd.: New York; 1975.
35. *Gmelin Handbuch der Anorganischen Chemie*, Selten Erden: Berlin; 1988, 9 - 11.
36. Ref. No. 35; 1988, 10, 1 - 20.
37. Glubkov, A.V.; Zhukova, T.B.; Sergeeva, V.M.; *Inorganic materials*, USSR; 1966, 2, 77 -81.

38. Nagai, S.I.; Shinemy, M.; Yokokawa, T.; *J. Inorganic Chemistry*, 1974, 36, 1904 - 1905.
39. Obolonchik, V.A.; Mikhlian, T.M.; *Inorganic Materials, USSR*; 1970, 6, 1385 - 1387.
40. Landelli, A.; *Z. Anorg. Allgem. chem.*, 1956, 288, 81 - 86.
41. Mahanti, S.D.; Kaplan, T.A.; Barma, M.; *J. Appl. Phys.* 1978, 49, 2084 - 2089.
42. Kaldis, E.; *Crystal Growth (Theory and Techniques)*, New York; 1974, 49 / 91.
43. Jayaraman, A.; *Handbook of Physics and chemistry of rare - earths*, Amsterdam; 1979, 2, 575 / 611.
44. Khan, A.; Manzi, L.; *Vapour Deposition Intern. Conf.*, Slough: London; 1975, 317 / 330.
45. Khan, A.; Vallaneilla, C.; *Vapour Deposition Intern. Conf.*, Slough: London; 1975, 331 / 43.
46. Jeffes, J.H.E.; Marples, T.N.R.; *J. Crystal Growth*, 1972, 17, 46 - 52.
47. Fenochka, B.V.; Gordienko, S.P.; *Russ. J. Phys. Chem.*, 1973, 47, 1384.
48. Ref. No. 35, 1988, 7, 25 - 35.
49. Mills, K.C.; *Thermodynamic Data for Inorganic Sulphides, Selenides, and Tellurides*, London; 1974, 471 / 81.
50. Ref. No. 35, 1968, 6, 1 - 5 / 132.
51. Hirayama, C.; Castle, P.M.; Liberman, R.W.; *Inorganic Chemistry*, 1974, 13, 2804 / 7.
52. Petzel, T.; Ludwings, J.; *High Temperature Science*, 1987, 24, 79 - 91.

53. Kuz'micheva, G.M.; Goryunov, A.V.; Elseev, A.A.; *Russ. J. Inorganic Chemistry*, 1987, 32, 632 - 636.
54. Karapytants, M.K.; *Chemical Thermodynamics*, Moscow; 1978, 604 - 624.
55. Brasted, R.C.; *Comprehensive Inorganic Chemistry*, New York; 1961, 8, 11-112.
56. Bichowsky, F.R.; Rossini, F.D.; *The Thermochemistry of the Chemical Substances*, New York; 1963, 17 / 170.
57. Bailar, J.C.; Emeleùs, H.J.; *Comprehensive Inorganic Chemistry*, 1975, 4, 1/100.
58. Sherwood, D.; *Introductory Chemical Thermodynamics*, Longman Group Ltd.; London: 1971, 119 / 190.
59. Swalin, R.A.; *Thermodynamics of Solids*, 2nd Edition, New York; 1972.
60. Koltz, I.M.; Rosenberg, R.M.; *Chemical Thermodynamics (Basic Theory and Methods)*, 5th Edition, New York; 1996.
61. Rosenberger, F.; *Fundamentals of Crystal Growth I*, New York; 1979.
62. Marx V.; Petzel, T.; *Journal of the Less-Common Metals*, 1990, 163, 199-207.
63. Tarjan, I.; Hatrai, M.; *Laboratory Manual on Crystal Growth*, Budapest; (1972).
64. Takashi, T.; *J. Crystal Growth*, 1970, 6, 319 - 322.
65. Agrawal, M.K.; Petel, P.D.; Gupta, J.K.; *J. Crystal Growth*, 1993, 128, 559-592.
66. Ganesha, R.; Arivouli, D.; Ramasamy, P.; *J. Crystal Growth*, 1993, 128, 1081 - 1085.
67. Keer, H.V.; *Principles of the Solid State*, Revised Edition, 1994, 15 -26.
68. West, A.R.; *Basic Solid State Chemistry*, 4th Edition, London; 1994, 137 - 139.
69. Kraus, H.; Noze, G.; *Powder Cell 1.8*, BAM, Berlin (Soft Ware Program).
70. Pearsall, T.; *J. Crystal Growth*, 1973, 20, 192 - 194.
71. Kyriakos, D.S.; Tarakostas, T.K.; Economou, N.A.; *J. Crystal Growth*, 1976,

- 35, 223 - 226.
72. Henry, N.F.M.; Lonsdale, K.; *International Tables for X - Ray crystallography*, London; 1962.
73. Wyckoff, R.W.G.; *Crystal Structures*, 2nd Edition, 1965, 1.
74. Akutagawa A.; Zanio, K.; *J. Crystal Growth*, 1971, 11, 191 - 196.
75. Landelli, A.; *Proc. of 1st Conf. Rare - Earth Research*, California; 1961, 135 - 41.
76. Gschneidner, K.A.; *Rare - earth Alloys*, New York; 1961.
77. Nachman, J.F.; Lundin, C.E.; *Rare - Earth Research*, 1961.
78. Rimmington, H.P.B.; Balchin, A.A.; Tanner, B.K.; *J. Crystal Growth*, 1972, 15, 51 - 56.
79. Parker, S.G.; *J. Crystal Growth*, 1971, 9, 177 - 182.
80. kodama, H.; Komatsu, H.; *J. Crystal Growth*, 1976, 36, 121 - 124.
81. Pribyl'skaya, N.Y.; Eliseev, A.A.; Pribyl'skii, N.Y.; Gamidov, R.S.; *Russ. Journal of Inorganic Chemistry*, 1984, 29, 451 - 453.
82. Rosenberger, F.; DeLong, M.C.; Olson, J.M.; *Journal of Crystal Growth*, 1973, 317 - 328.
83. Udea, R.; Mullin, J.B.; *Crystal Growth and Characterization*, 1975, 243 -256.

Appendix 57-I: Listing of Pascal Program

```
program GRAT06;
{$N+}
uses
  Crt, Graph, Q3BU2;

label
  L1;

var
  HfZcl, HfZnS, hfCl, HfS, HR: Double;
  CpZCl, CpS, CpZns, CpCl, CpR: Double;
  HRT1, HRT2, SZCl, SS, SZnS, SCI, SR: Double;
  SRT1, SRT2, T1, T2, GT1, GT2, Keq1, Keq2, RG: Double;
  PZnCl1, PZnCl2, PS, PCl, PZnS : Double;
  CPA, CPB, CPC: Double;
  Root1, Root2, lnPZnCl1, lnPZnCl2, DeltaP: Double;
  Sp1, Sp2, moll2, PI2: Double;
  reaction, Name: String;
  StrHfZnS, StrHfCl, StrHfZcl, StrHfS: String;
  StrSZnS, StrSCI, StrSZcl, StrSS, StrCpA, StrCpB, StrCpC: String;
  StrMoll2: String;
  m, n: Integer;
  Color: Word;
  GraphDriver, GraphMode: Integer;
  pin1, pin2, r, s, t, p, q, y: Double;
```

```
procedure SchrT(Fz: Byte; Ox: Byte; Oy: Byte; Txt: string);
begin
  Textcolor(Fz);
  GotoXY(Ox, Oy);
  Write(Txt);
end;
```

```
begin
  TextBackground(1);
  ClrScr;
  Write('Name of File e.g. ZNS.BIT  : ');
  Readln(Name);
  Write('Reaction e.g. ZnS + Cl2 = ZnCl2 + 0.5 S2 : ');
  Readln(reaction);
  Write('delta Hf298 MeCha e.g. ZnS  : ');
  Readln(HfZnS);
  Write('delta Hf298 Hal2 e.g. Cl2  : ');
  Readln(HfCl);
  Write('delta Hf298 MeHal2 e.g. ZnCl2 : ');
  Readln(HfZcl);
  Write('delta Hf298 Cha2 e.g. S2  : ');
  Readln(HfS);
  Write('delta S298 MeCha e.g. ZnS  : ');
  Readln(SZnS);
  Write('delta S298 Hal2 e.g. Cl2  : ');
  Readln(SCI);
  Write('delta S298 MeHal2 e.g. ZnCl2 : ');
  Readln(SZcl);
  Write('delta S298 Cha2 e.g. S2  : ');
  Readln(SS);
  Write('CpA          : ');
```

```

Readln(CpA);
Write('CpB           ');
Readln(CpB);
Write('CpC           ');
Readln(CpC);
Write('I2 in mol/cm3 ');
Readln(moll2);
HR:=HfZCl+0.5*HfS-HfZnS-HfCl;
SR:=SZCl+0.5*SS-SZnS-SCI;
RG:=8.314;

```

```

GraphDriver:=9; GraphMode:=2;
InitGraph(GraphDriver, GraphMode, '\TP\BGI');
SetBkColor(0);
QLaden('CTR-EMT6.BIT');
Str(moll2:8:6,StrMoll2);
Str(HfZnS:6:2,StrHfZnS);
Str(HfCl:6:2,StrHfCl);
Str(HfZcl:6:2,StrHfZcl);
Str(HfS:6:2,StrHfS);
Str(SZnS:6:2,StrSZnS);
Str(SCl:6:2,StrSCl);
Str(SZcl:6:2,StrSZcl);
Str(SS:6:2,StrSS);
Str(CpA:10:8,StrCpA);
Str(CpB:10:8,StrCpB);
Str(CpC:10:8,StrCpC);
SetTextStyle(2,0,5);
SetColor(5);
OutTextXY(10,24,reaction);
SetTextStyle(2,0,4);
SetColor(4);
OutTextXY(80,42,StrMoll2);
OutTextXY(80,62,StrHfZnS);
OutTextXY(80,82,StrHfCl);
OutTextXY(80,102,StrHfZcl);
OutTextXY(80,122,StrHfS);
OutTextXY(80,142,StrSZnS);
OutTextXY(80,162,StrSCl);
OutTextXY(80,182,StrSZcl);
OutTextXY(80,202,StrSS);
OutTextXY(70,222,StrCpA);
OutTextXY(70,237,StrCpB);
OutTextXY(70,252,StrCpC);
For m:=0 to 400 do begin
  T1:=300+2.5*m;
  pin1:=moll2*0.08206*T1*1000;
  For n:=0 to 400 do begin
    T2:=300+2.5*n;
    pin2:=moll2*0.08206*T2*1000;
    If pin1 > 1.333 then begin
      Color:=8;
      GoTo L1;
    end;
    If pin2 > 1.333 then begin
      Color:=8;
      GoTo L1;
    end;
    HRT1:=HR+0.001*((CpA*T1+(CpB/2)*T1*T1+CpC/(T1*T1))-
(CpA*298+(CpB/2)*298*298+CpC/(298*298)));

```

```

HRT2:=HR+0.001*((CPA*T2+(CPB/2)*T2*T2+CPC/(T2*T2))-
(CPA*298+(CPB/2)*298*298+CPC/(298*298)));
SRT1:=SR+((CPA*ln(T1)+Cpb*T1-0.5*Cpc/(T1*T1))-((CPA*Ln(298)+cpB*298-
0.5*cPC/(298*298))));
SRT2:=SR+((CPA*ln(T2)+Cpb*T2-0.5*Cpc/(T2*T2))-((CPA*Ln(298)+cpB*298-
0.5*cPC/(298*298))));
GT1:=HRT1-T1*SRT1*0.001;
GT2:=HRT2-T2*SRT2*0.001;
Keq1:=exp((-GT1*1000)/(RG*T1));
Keq2:=exp((-GT2*1000)/(RG*T2));

```

{Cardano-Prozedur}

```

r:=-4*Keq1*Keq1;
s:=8*Keq1*Keq1*pin1;
t:=-4*Keq1*Keq1*pin1*pin1;
p:=s-(r*r)/3;
q:=((2*r*r*r)/27)-((r*s)/3)+t;
If 0 < ((q/2)*(q/2))+((p/3)*(p/3)*(p/3)) then begin
If (-q/2)+SQRT(((q/2)*(q/2))+((p/3)*(p/3)*(p/3))) > 0 then begin
Root1:=ln((-q/2)+SQRT(((q/2)*(q/2))+((p/3)*(p/3)*(p/3))))/3;
Root1:=exp(Root1);
end;
If (-q/2)+SQRT(((q/2)*(q/2))+((p/3)*(p/3)*(p/3))) < 0 then begin
Root1:=ln(-(-q/2)+SQRT(((q/2)*(q/2))+((p/3)*(p/3)*(p/3))))/3;
Root1:=-exp(Root1);
end;
If (-q/2)-SQRT(((q/2)*(q/2))+((p/3)*(p/3)*(p/3))) > 0 then begin
Root2:=ln((-q/2)-SQRT(((q/2)*(q/2))+((p/3)*(p/3)*(p/3))))/3;
Root2:=exp(Root2);
end;
If (-q/2)-SQRT(((q/2)*(q/2))+((p/3)*(p/3)*(p/3))) < 0 then begin
Root2:=ln(-(-q/2)-SQRT(((q/2)*(q/2))+((p/3)*(p/3)*(p/3))))/3;
Root2:=-exp(Root2);
end;
y:=Root1+Root2;
pZnCl1:=y-(r/3);
end;
If 0 >= ((q/2)*(q/2))+((p/3)*(p/3)*(p/3)) then begin
Color:=7;
Goto L1;
end;

```

```

r:=-4*Keq2*Keq2;
s:=8*Keq2*Keq2*pin2;
t:=-4*Keq2*Keq2*pin2*pin2;
p:=s-(r*r)/3;
q:=((2*r*r*r)/27)-((r*s)/3)+t;
If 0 < ((q/2)*(q/2))+((p/3)*(p/3)*(p/3)) then begin
If (-q/2)+SQRT(((q/2)*(q/2))+((p/3)*(p/3)*(p/3))) > 0 then begin
Root1:=ln((-q/2)+SQRT(((q/2)*(q/2))+((p/3)*(p/3)*(p/3))))/3;
Root1:=exp(Root1);
end;
If (-q/2)+SQRT(((q/2)*(q/2))+((p/3)*(p/3)*(p/3))) < 0 then begin
Root1:=ln(-(-q/2)+SQRT(((q/2)*(q/2))+((p/3)*(p/3)*(p/3))))/3;
Root1:=-exp(Root1);
end;
If (-q/2)-SQRT(((q/2)*(q/2))+((p/3)*(p/3)*(p/3))) > 0 then begin
Root2:=ln((-q/2)-SQRT(((q/2)*(q/2))+((p/3)*(p/3)*(p/3))))/3;
Root2:=exp(Root2);
end;
If (-q/2)-SQRT(((q/2)*(q/2))+((p/3)*(p/3)*(p/3))) < 0 then begin

```

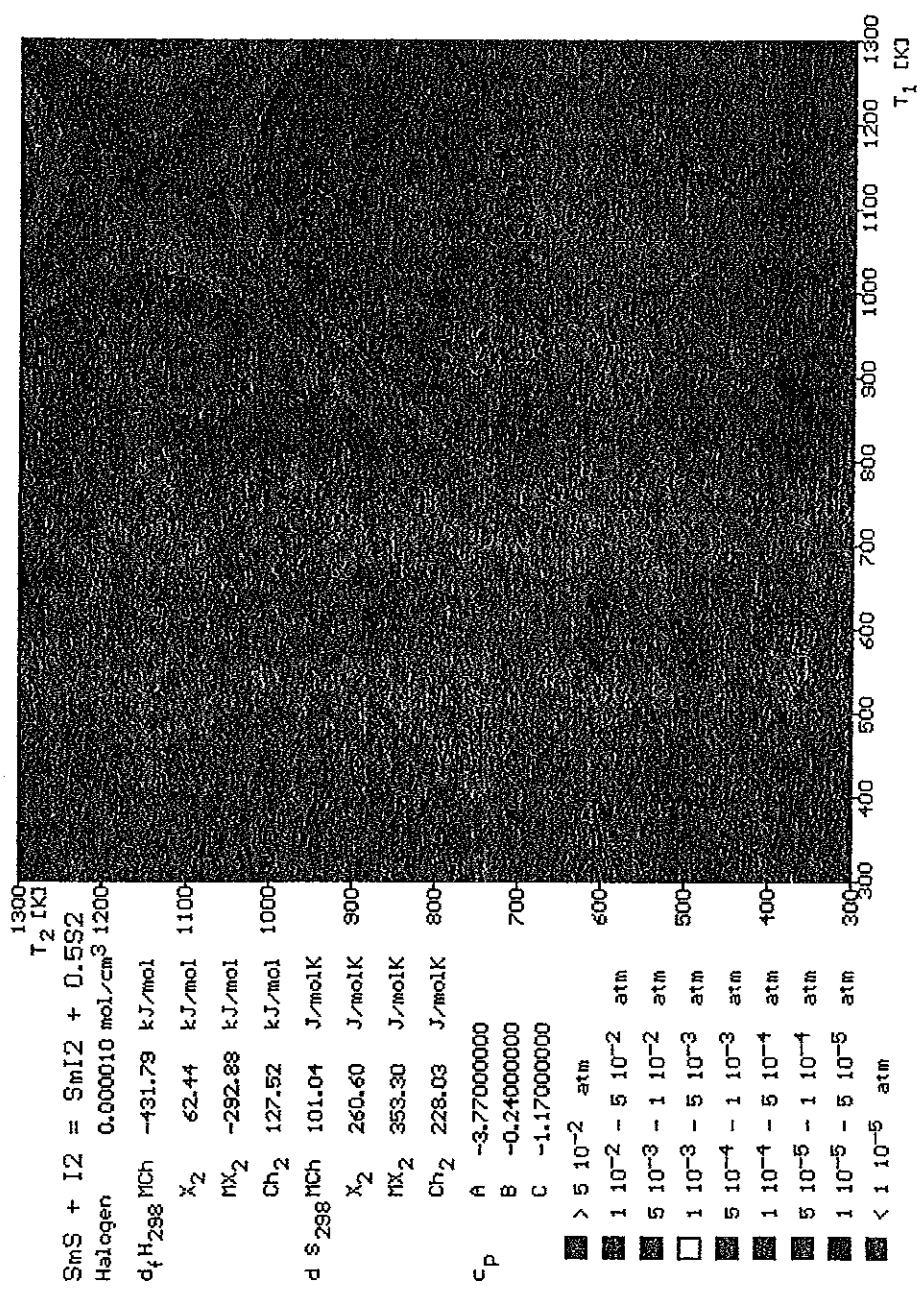
```

Root2:=ln(-((-q/2)-SQRT(((q/2)*(q/2))+((p/3)*(p/3)*(p/3)))))/3;
Root2:=-exp(Root2);
end;
y:=Root1+Root2;
pZnCl2:=y-(r/3);
end;
If 0 >= ((q/2)*(q/2))+((p/3)*(p/3)*(p/3)) then begin
  Color:=7;
  Goto L1;
end;

DeltaP:=PZnCl2-PZnCl1;
DeltaP:=Abs(DeltaP);
If DeltaP >= 5E-2 then Color:=13;
If DeltaP < 5E-2 then Color:=4;
If DeltaP < 1E-2 then Color:=12;
If DeltaP < 5E-3 then Color:=14;
If DeltaP < 1E-3 then Color:=10;
If DeltaP < 5E-4 then Color:=2;
If DeltaP < 1E-4 then Color:=11;
If DeltaP < 5E-5 then Color:=3;
If DeltaP < 1E-5 then Color:=9;

L1:
  If T1 <> T2 then PutPixel(200+m,405-n,Color);
  end;
end;
QSpeicher(Name);
CloseGraph;
end.

```



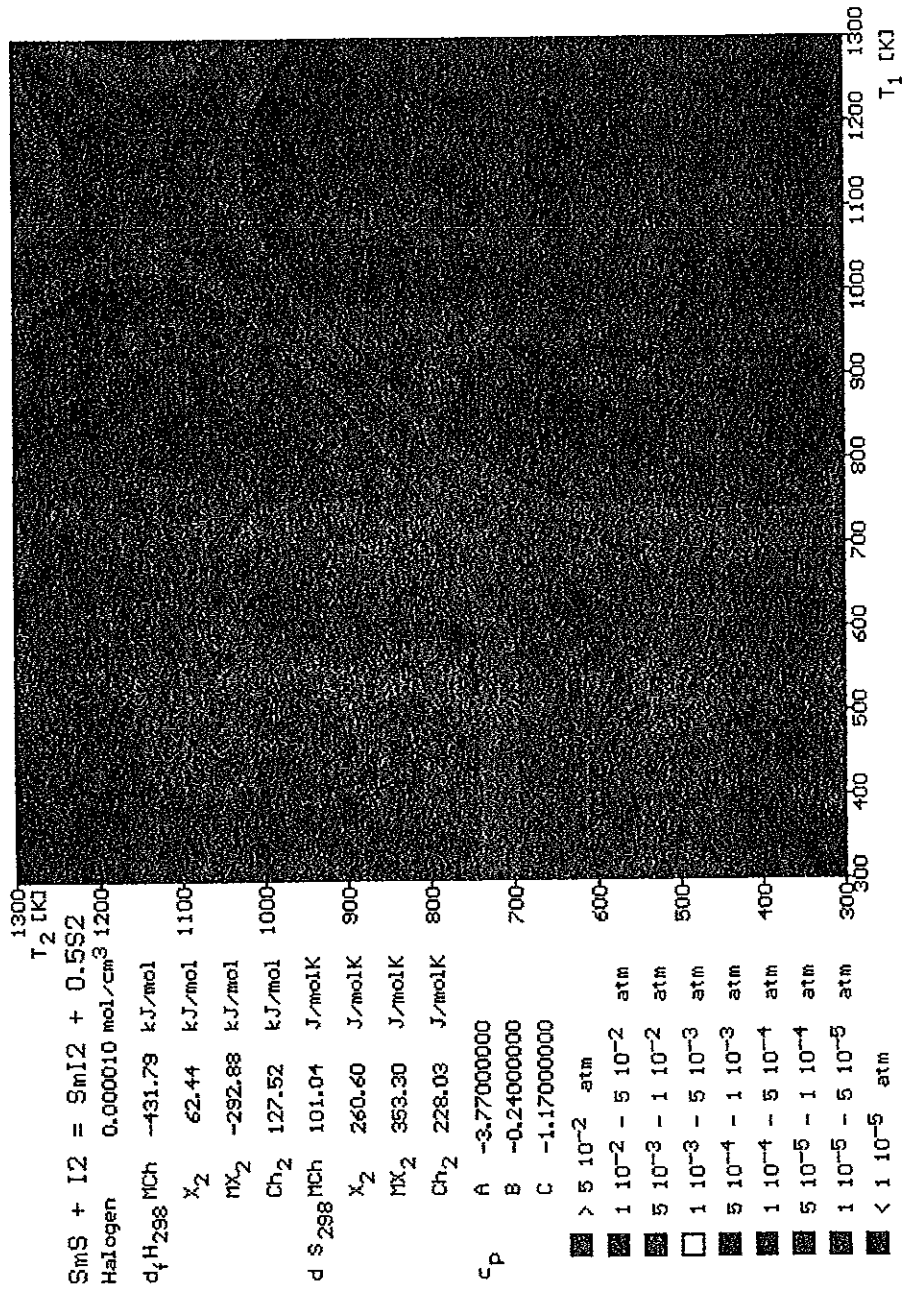
1300
T₂ [K]

SmS + I₂ = SmI₂ + 0.5S₂
 Halogen 0.000010 mol/cm³ 1200
 d_fH₂₉₈ MCh -431.79 kJ/mol
 X₂ 62.44 kJ/mol 1100
 MX₂ -292.88 kJ/mol
 Ch₂ 127.52 kJ/mol 1000
 d S₂₉₈ MCh 101.04 J/molK
 X₂ 260.60 J/molK 900
 MX₂ 353.30 J/molK
 Ch₂ 228.03 J/molK 800
 c_p A -3.77000000
 B -0.24000000
 C -1.17000000

600
500
400
300
T₁ [KJ]

> 5 10⁻² atm
 1 10⁻² - 5 10⁻² atm
 5 10⁻³ - 1 10⁻² atm
 1 10⁻³ - 5 10⁻³ atm
 5 10⁻⁴ - 1 10⁻³ atm
 1 10⁻⁴ - 5 10⁻⁴ atm
 5 10⁻⁵ - 1 10⁻⁴ atm
 1 10⁻⁵ - 5 10⁻⁵ atm
 < 1 10⁻⁵ atm

APPENDIX 55-II: SmS with I₂



1300
T₂ [K]

SmS + I₂ = SmI₂ + 0.5S₂

Halogen 0.000010 mol/cm³ 1200

d_fH₂₉₈ MCh -431.79 kJ/mol

X₂ 62.44 kJ/mol 1100

MX₂ -292.88 kJ/mol

Ch₂ 127.52 kJ/mol 1000

d S₂₉₈ MCh 101.04 J/molK

X₂ 260.60 J/molK 900

MX₂ 353.30 J/molK

Ch₂ 228.03 J/molK 800

c_p A -3.77000000

B -0.24000000

C -1.17000000

> 5 10⁻² atm

1 10⁻² - 5 10⁻² atm

5 10⁻³ - 1 10⁻² atm

1 10⁻³ - 5 10⁻³ atm

5 10⁻⁴ - 1 10⁻³ atm

1 10⁻⁴ - 5 10⁻⁴ atm

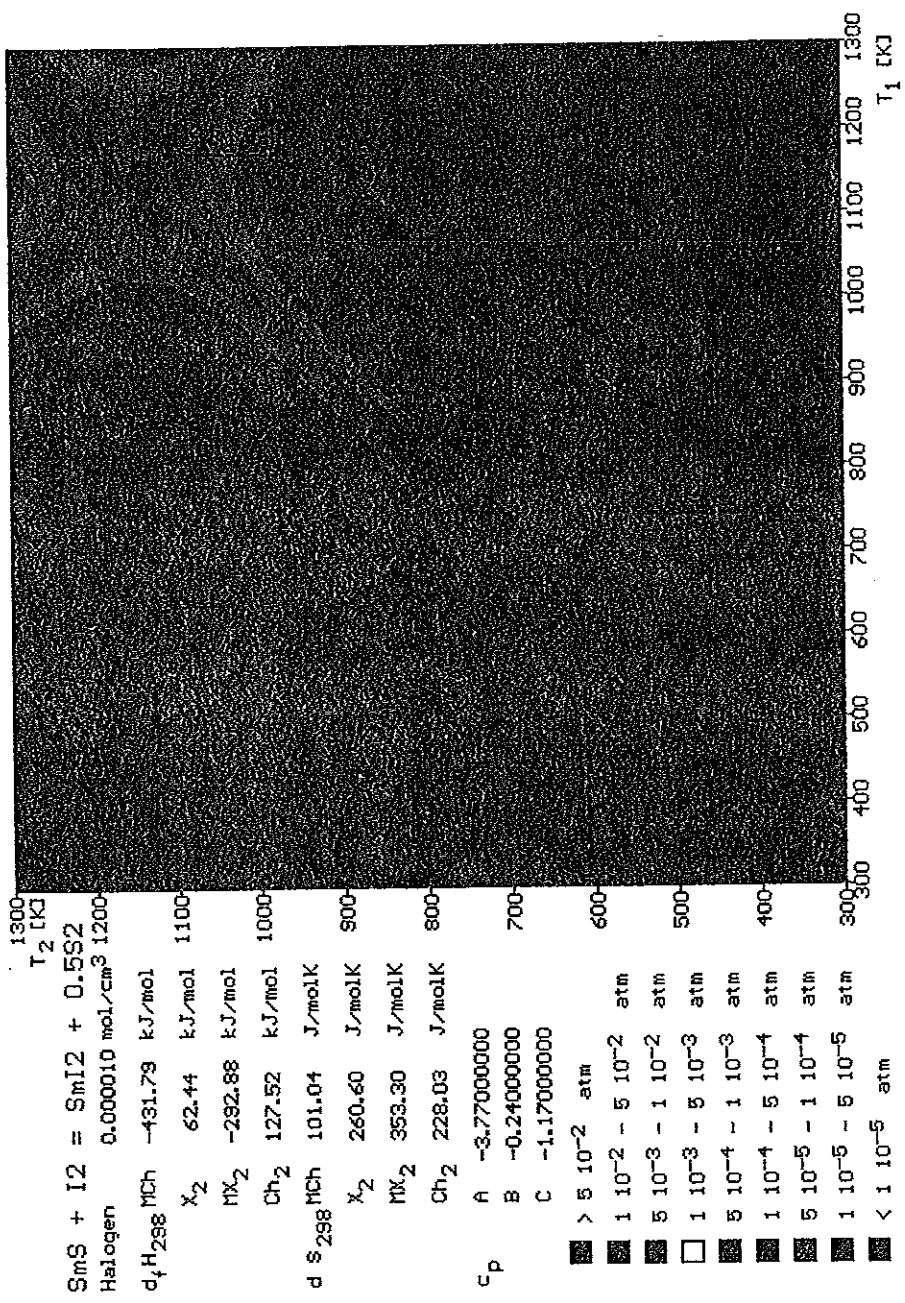
5 10⁻⁵ - 1 10⁻⁴ atm

1 10⁻⁵ - 5 10⁻⁵ atm

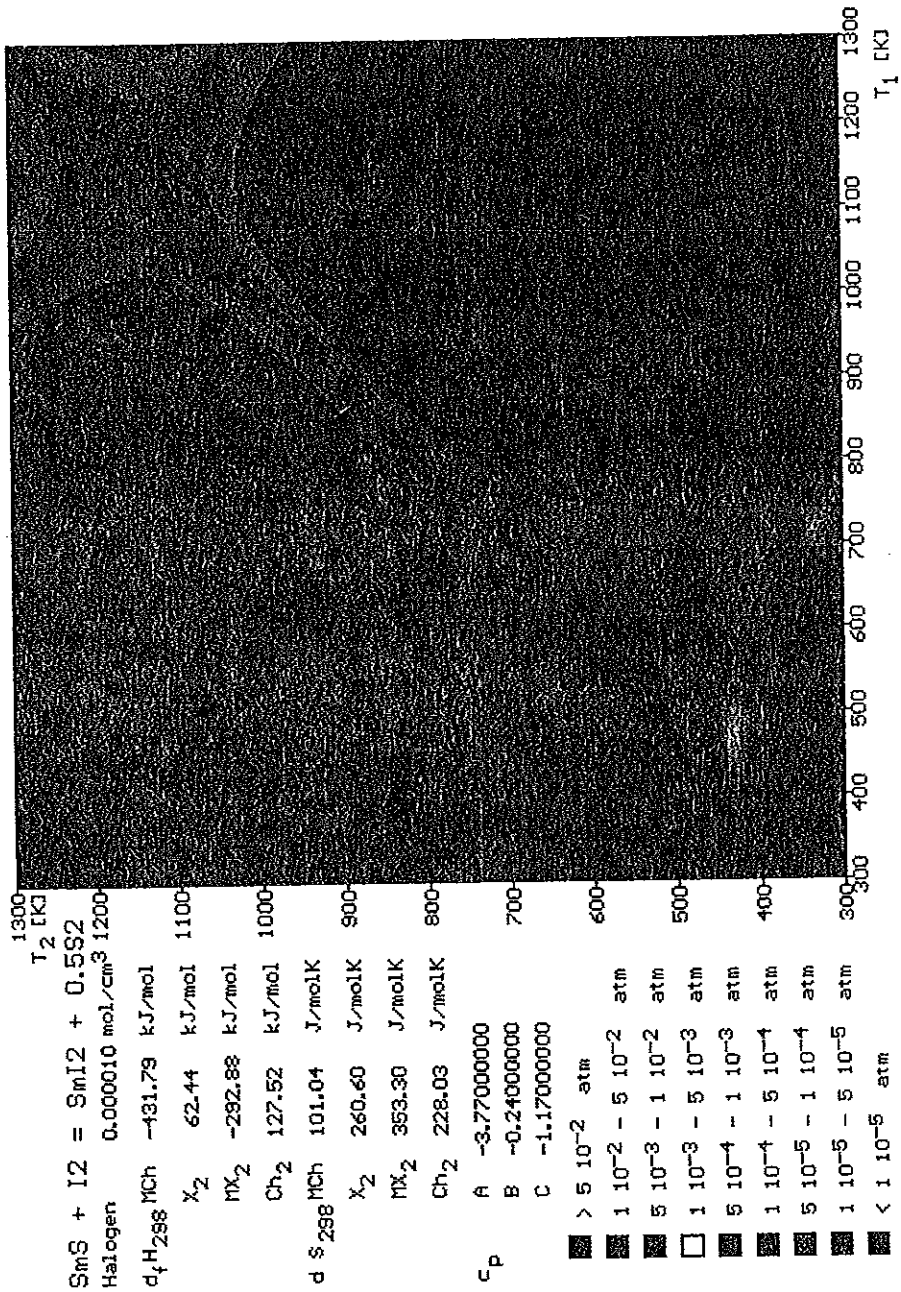
< 1 10⁻⁵ atm

300 400 500 600 700 800 900 1000 1100 1200 1300
T₁ [K]

APPENDIX 55-II: SmS with I₂



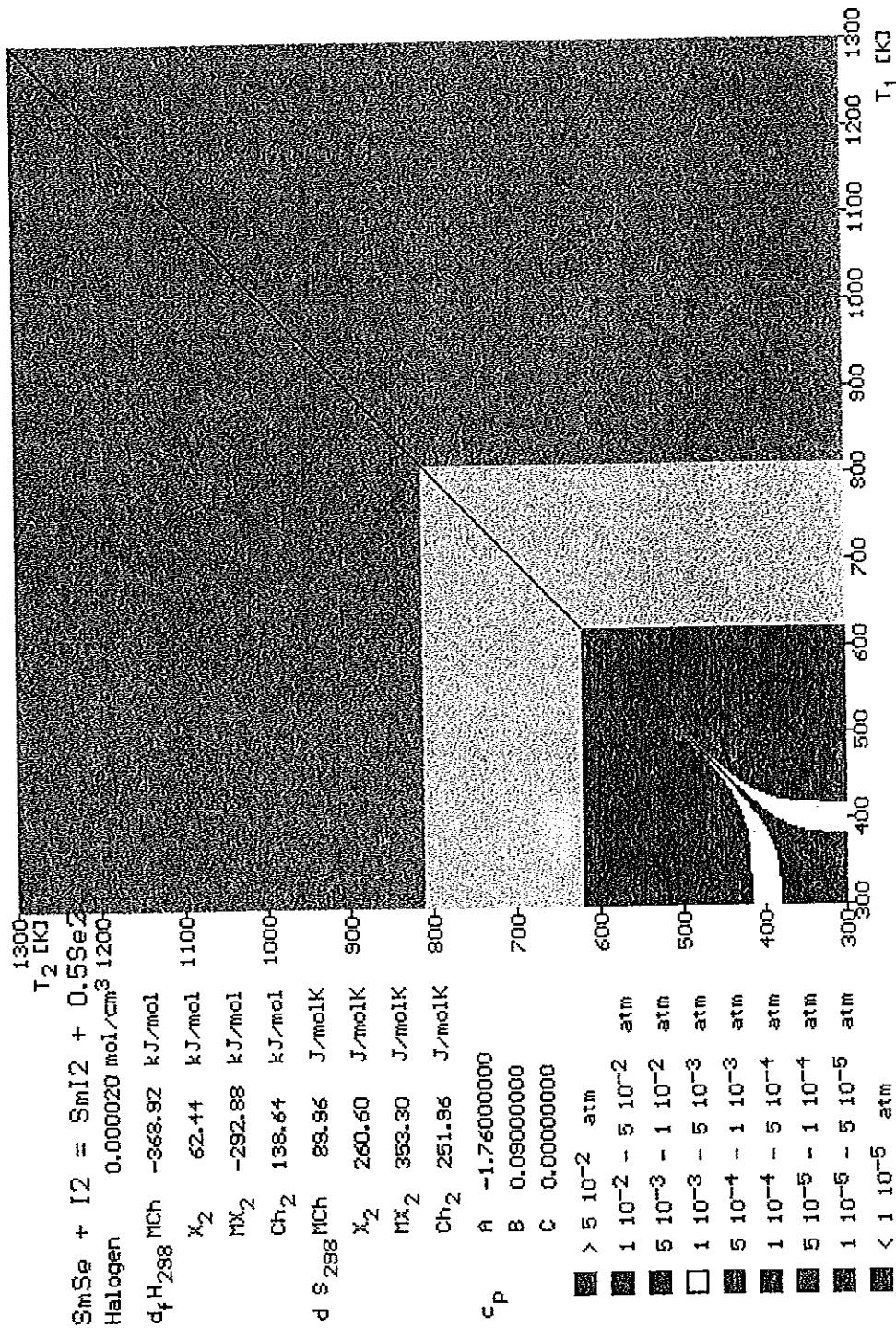
APPENDIX 55-II: SmS with I₂



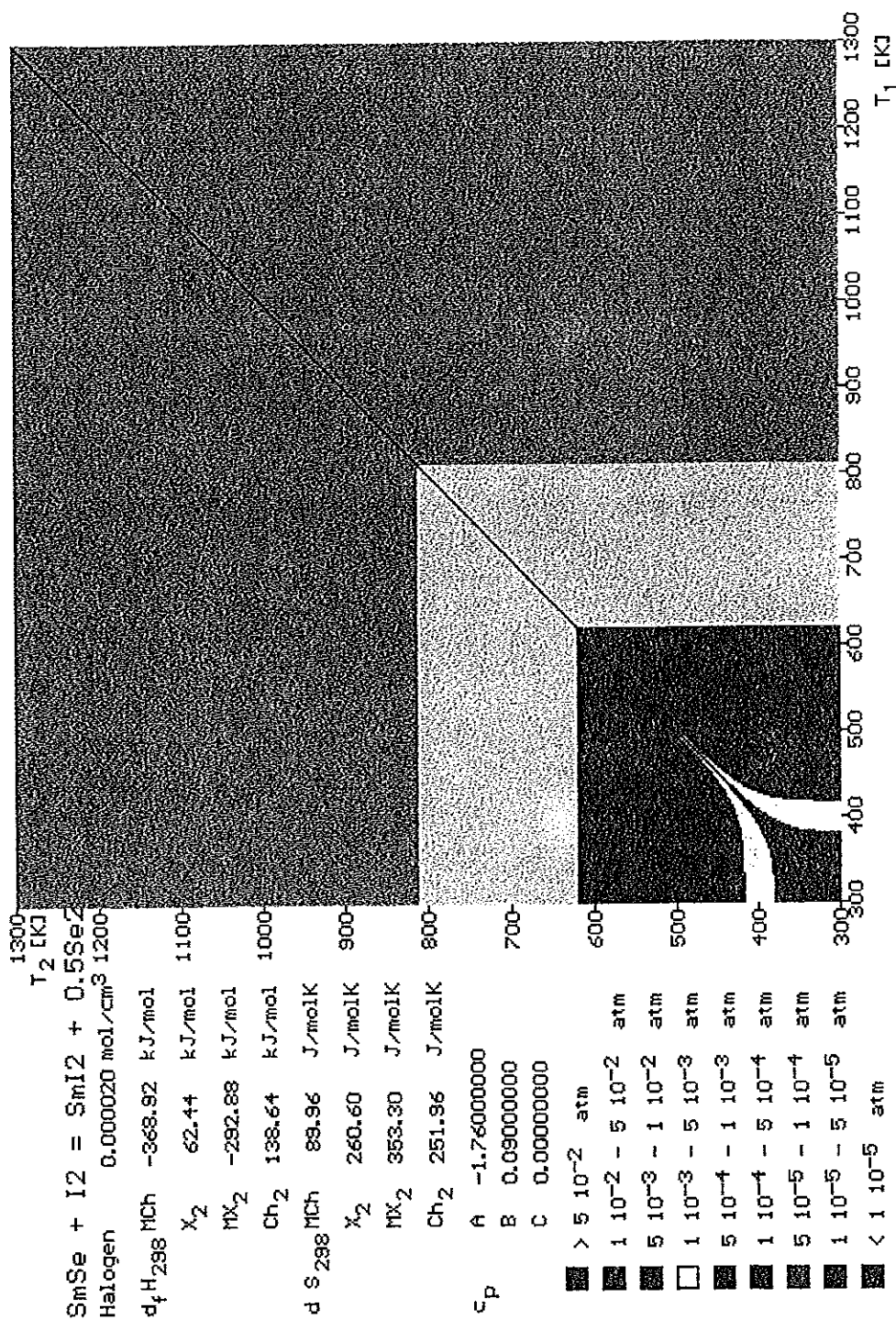
$SmI_2 + I_2 = SmI_2 + 0.5S_2$
 Halogen $0.000010 \text{ mol/cm}^3$ 1200
 $d_f H_{298} \text{ MCh}$ -431.79 kJ/mol
 X_2 62.44 kJ/mol 1100
 MX_2 -292.88 kJ/mol
 Ch_2 127.52 kJ/mol 1000
 $d S_{298} \text{ MCh}$ 101.04 J/molK
 X_2 260.60 J/molK 900
 MX_2 353.30 J/molK
 Ch_2 228.03 J/molK 800
 c_p A -3.77000000 700
 B -0.24000000
 C -1.17000000 600

- > $5 \cdot 10^{-2}$ atm
- $1 \cdot 10^{-2} - 5 \cdot 10^{-2}$ atm
- $5 \cdot 10^{-3} - 1 \cdot 10^{-2}$ atm
- $1 \cdot 10^{-3} - 5 \cdot 10^{-3}$ atm
- $5 \cdot 10^{-4} - 1 \cdot 10^{-3}$ atm
- $1 \cdot 10^{-4} - 5 \cdot 10^{-4}$ atm
- $5 \cdot 10^{-5} - 1 \cdot 10^{-4}$ atm
- $1 \cdot 10^{-5} - 5 \cdot 10^{-5}$ atm
- < $1 \cdot 10^{-5}$ atm

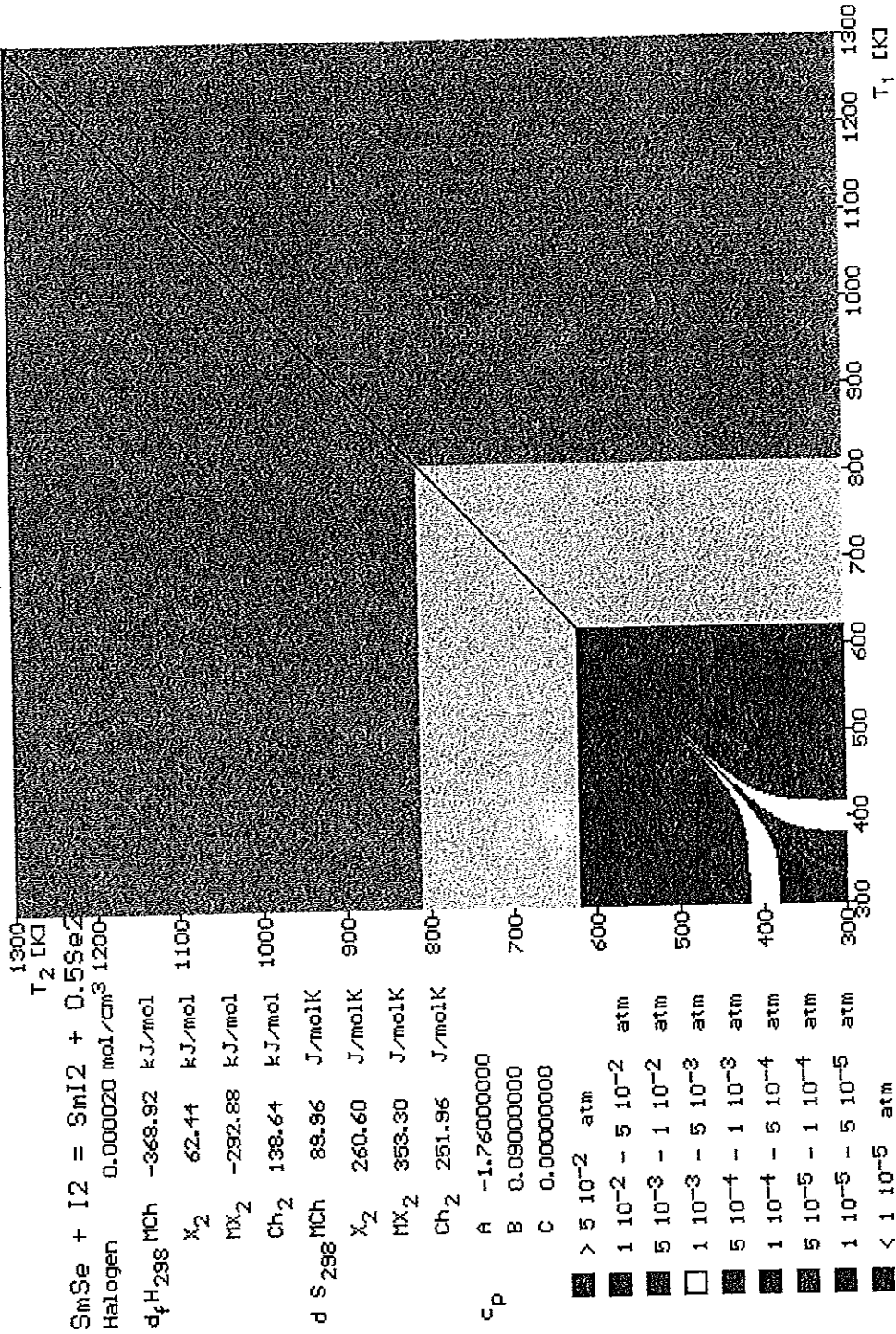
APPENDIX 55-U: SmS with I_2



APPENDIX 55-II: SmSe with I_2



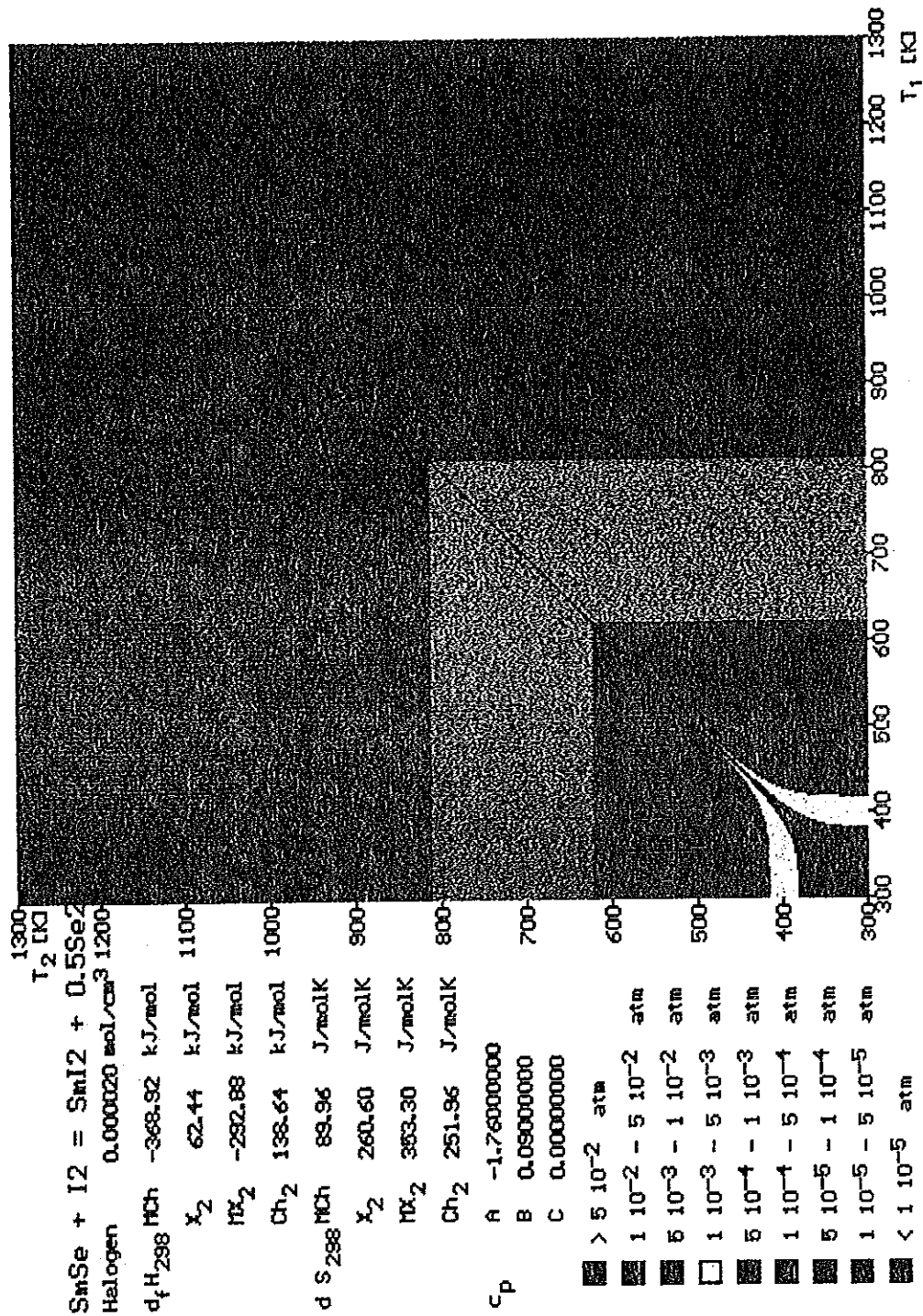
APPENDIX 55-II: SmSe with I_2



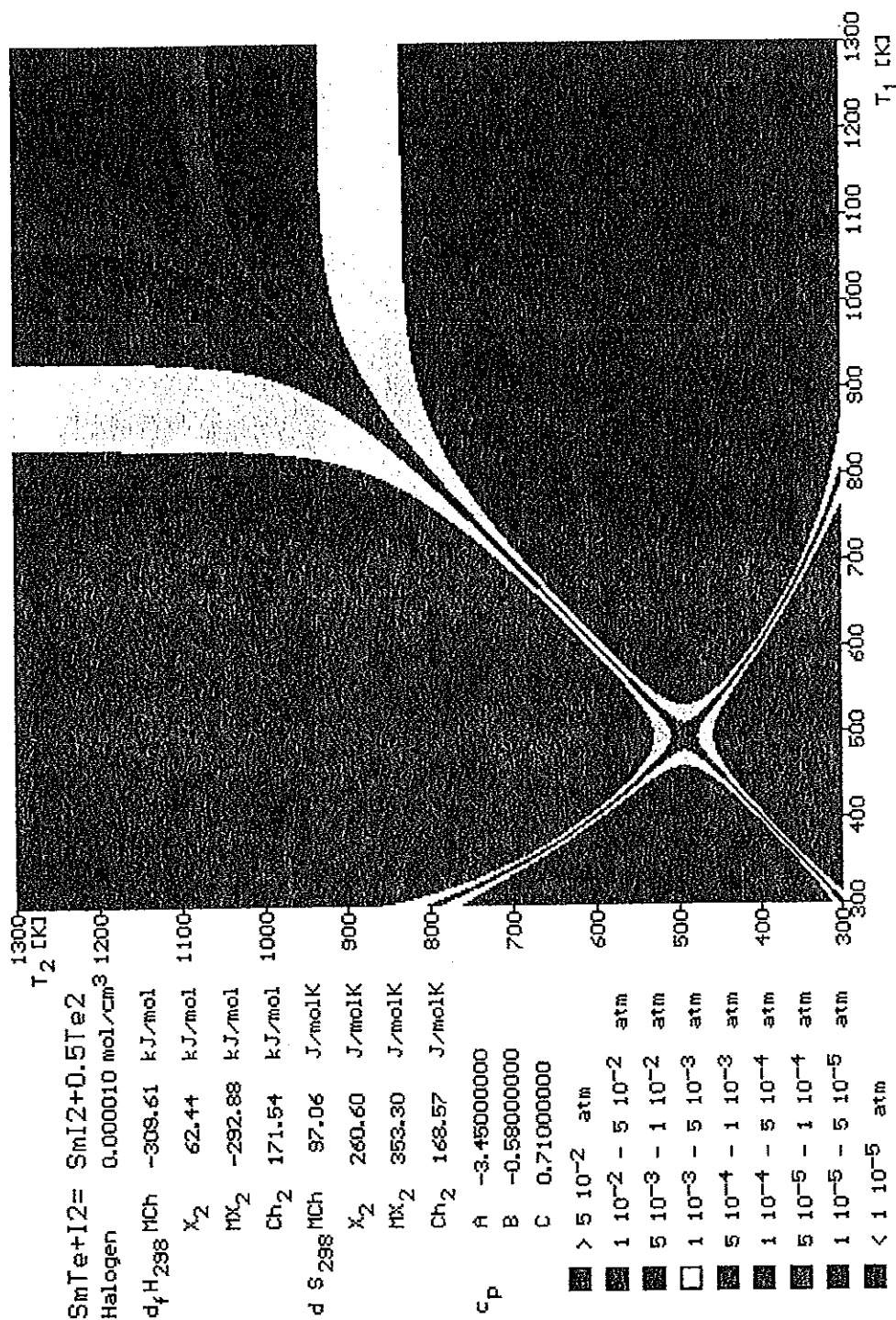
$\text{SmSe} + \text{I}_2 = \text{SmI}_2 + 0.5\text{Se}_2$
 Halogen 0.000020 mol/cm³ 1200-
 $d_f \text{H}_{298}$ MCh -368.92 kJ/mol
 X_2 62.44 kJ/mol 1100-
 MX_2 -292.88 kJ/mol
 Ch_2 138.64 kJ/mol 1000-
 $d \text{S}_{298}$ MCh 88.96 J/molK
 X_2 260.60 J/molK 900-
 MX_2 353.30 J/molK
 Ch_2 251.96 J/molK 800-
 c_p A -1.76000000
 B 0.09000000
 C 0.00000000

- > 5 10⁻² atm
- 1 10⁻² - 5 10⁻² atm
- 5 10⁻³ - 1 10⁻² atm
- 1 10⁻³ - 5 10⁻³ atm
- 5 10⁻⁴ - 1 10⁻³ atm
- 1 10⁻⁴ - 5 10⁻⁴ atm
- 5 10⁻⁵ - 1 10⁻⁴ atm
- 1 10⁻⁵ - 5 10⁻⁵ atm
- < 1 10⁻⁵ atm

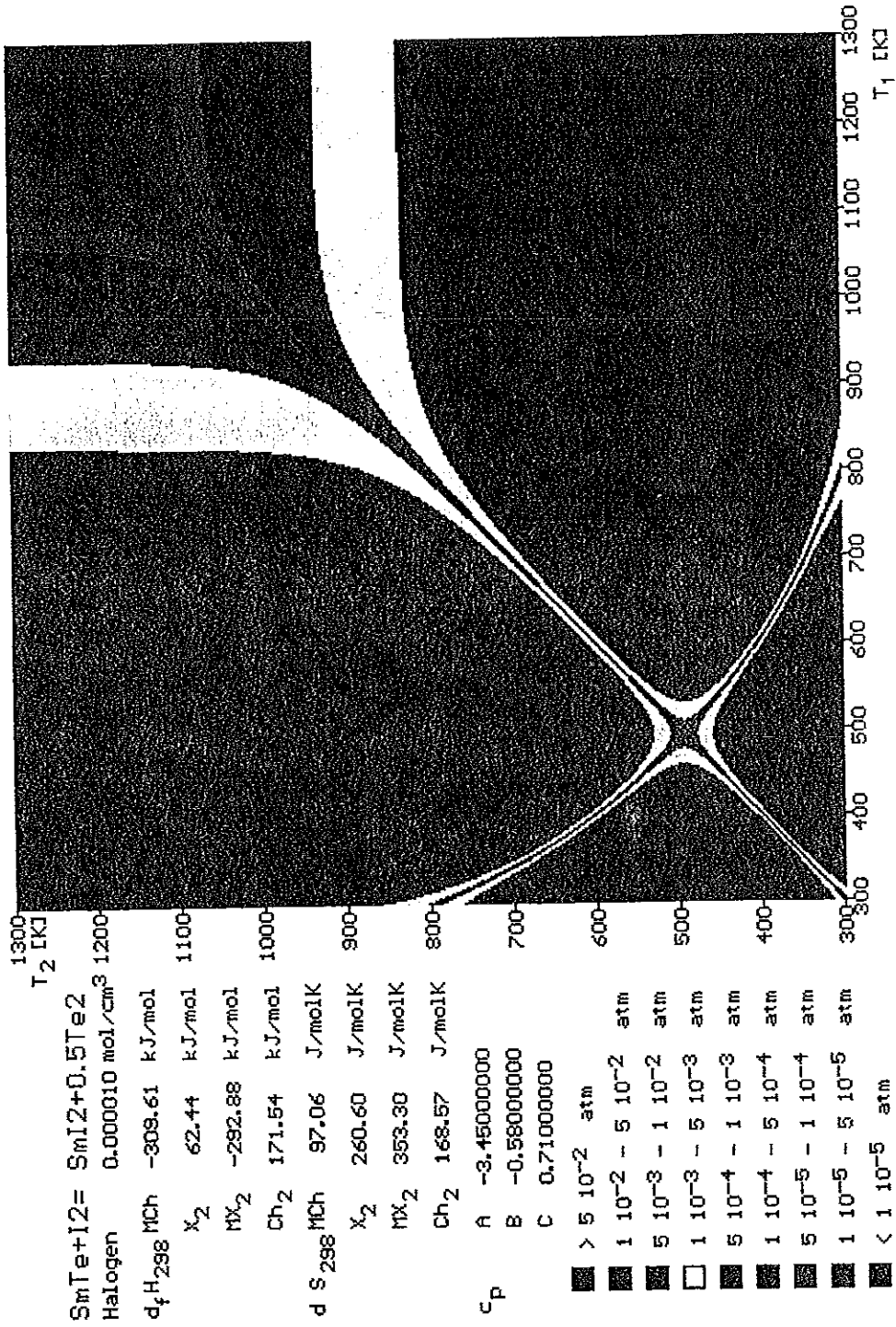
APPENDIX 55-II: SmSe with I₂



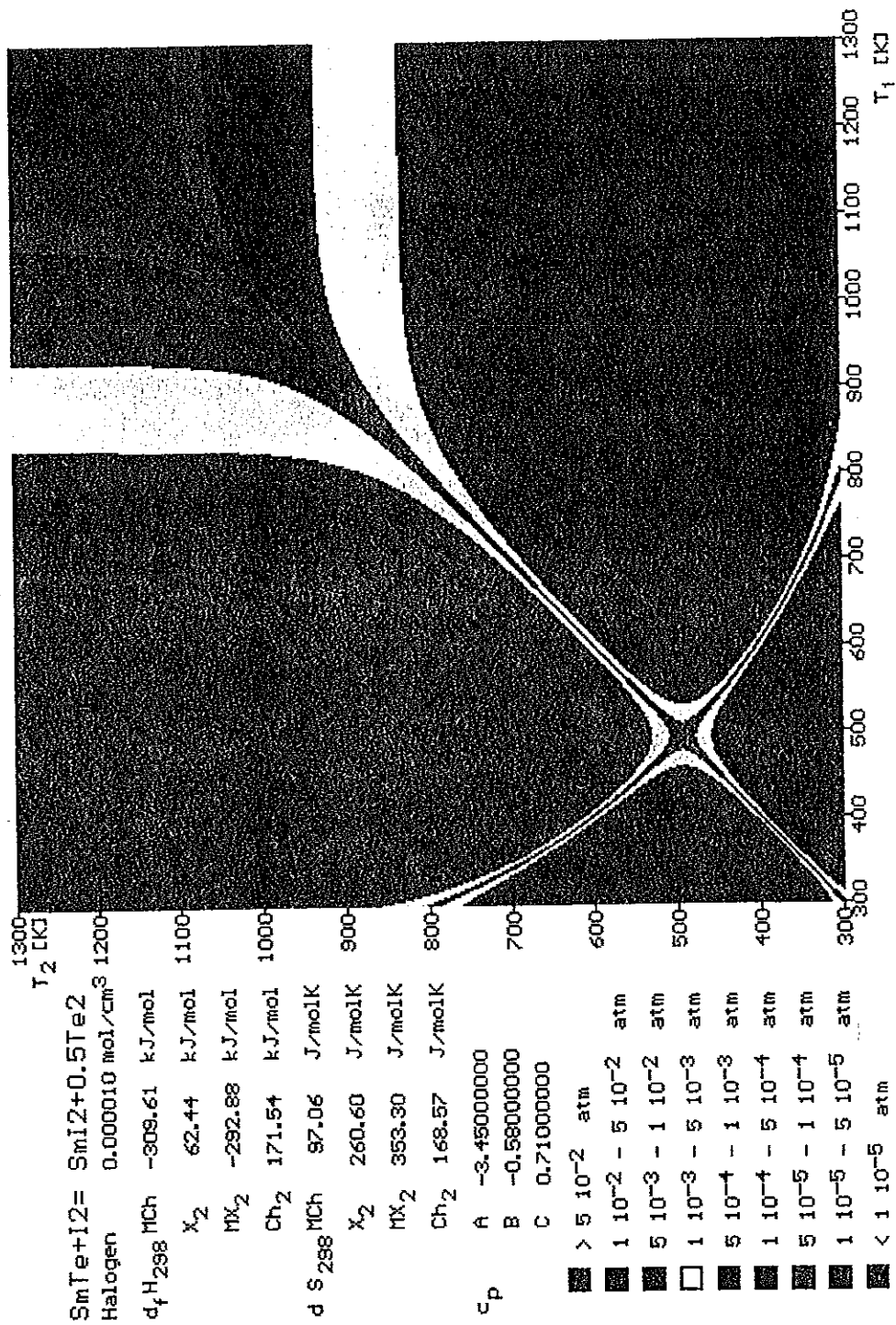
APPENDIX 57-II: SmSe with I_2



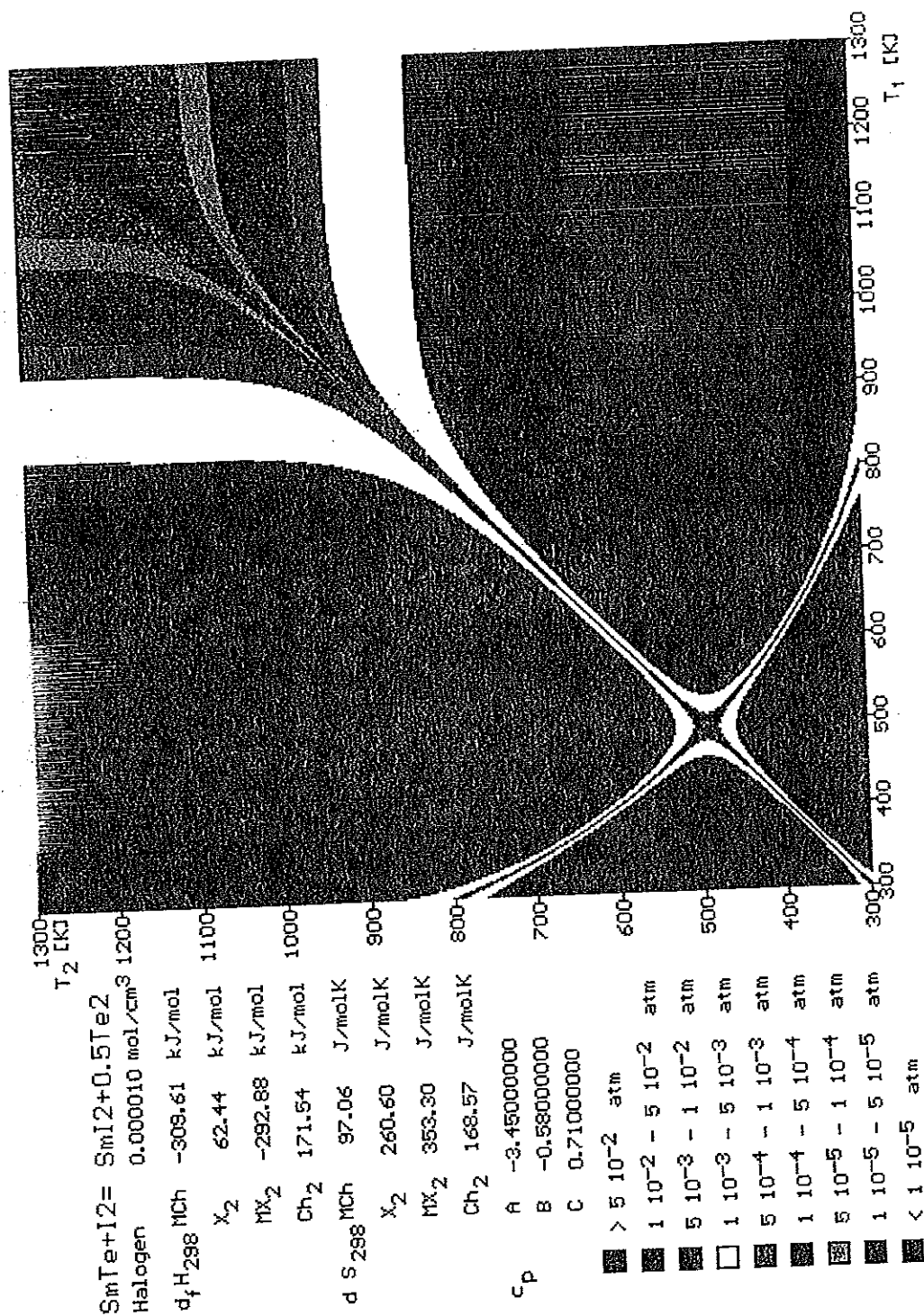
APPENDIX 55-II: SmTe with I_2



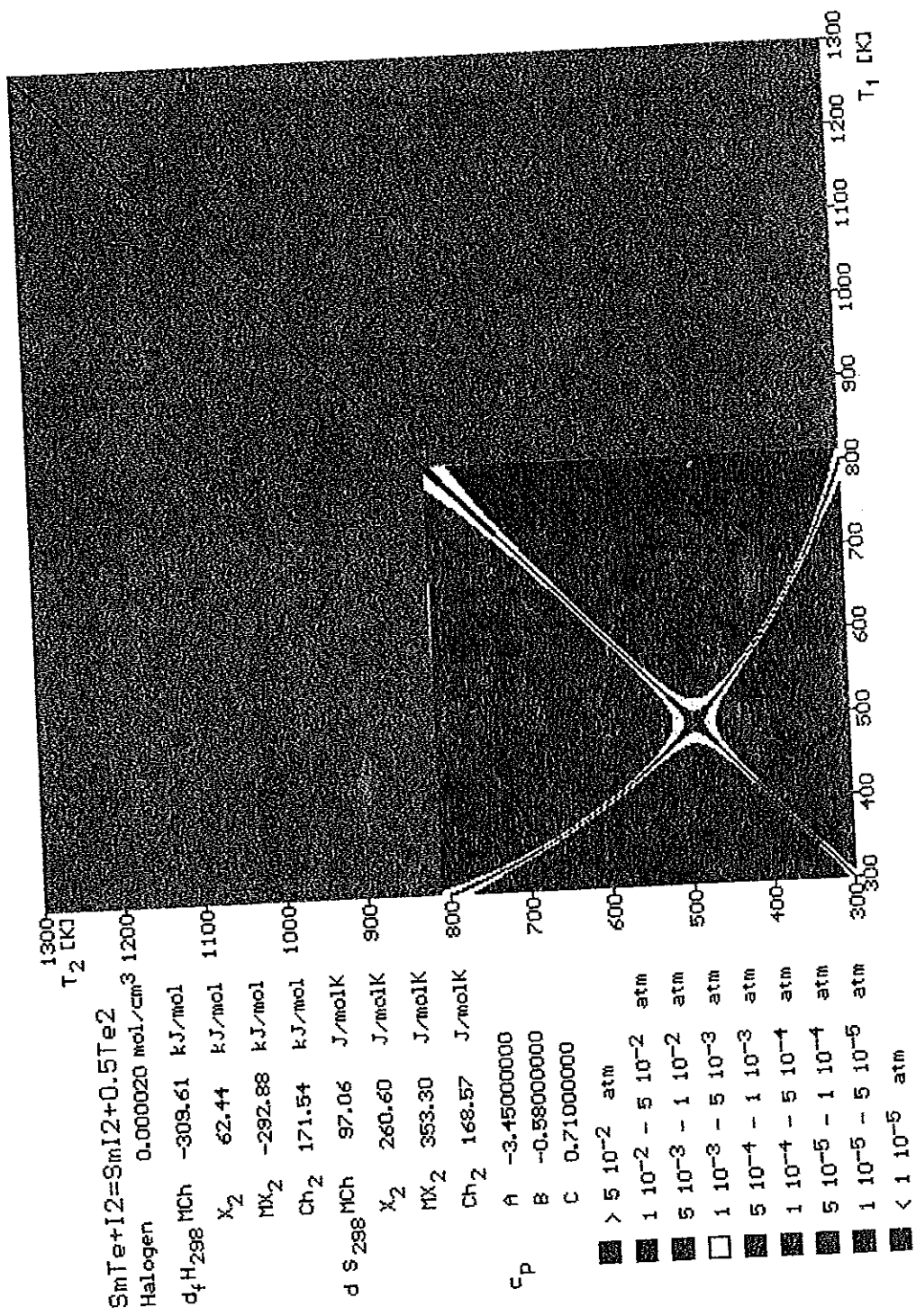
APPENDIX 55-II: SmTe with I₂



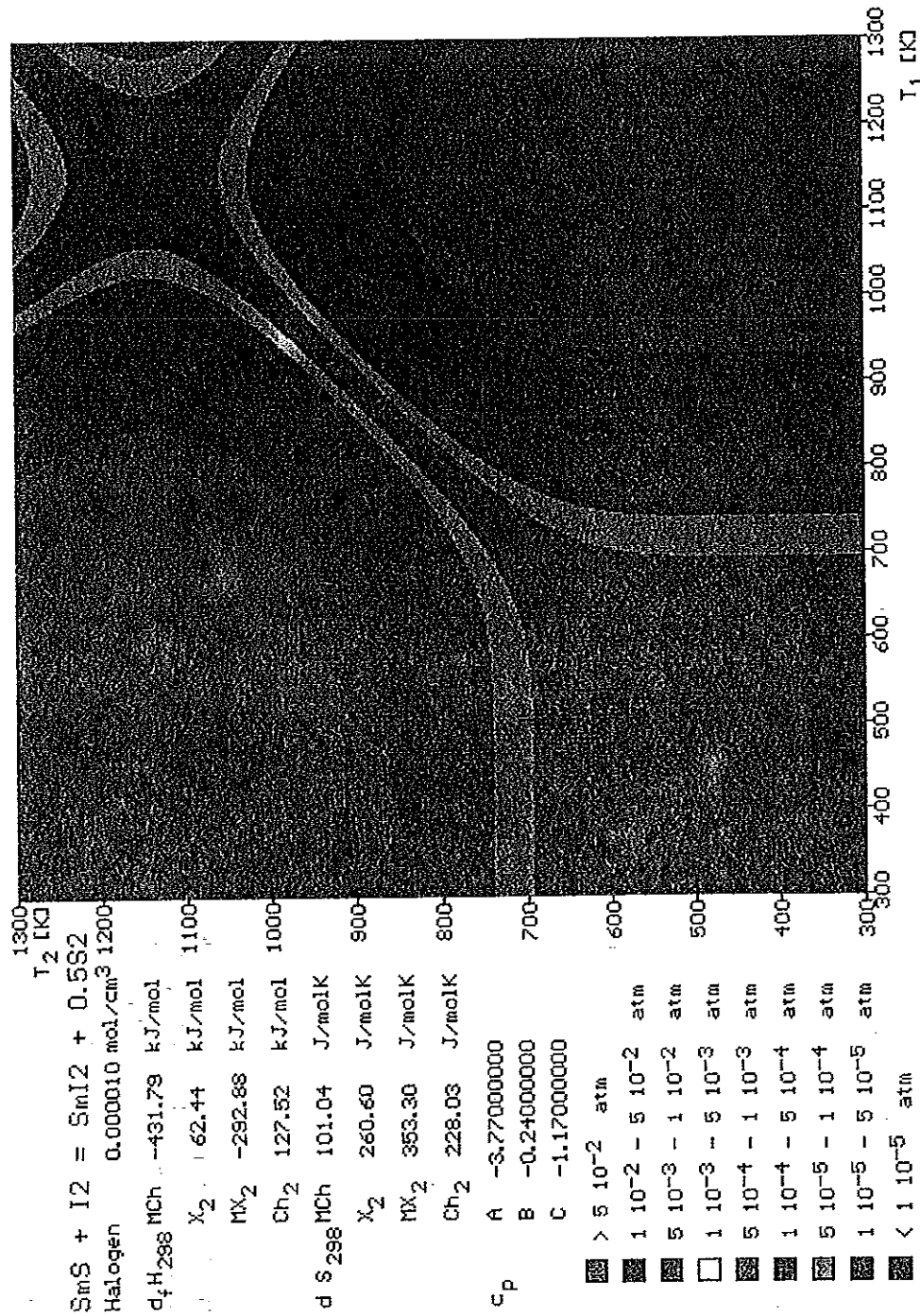
APPENDIX 55-II: SmTe with I₂



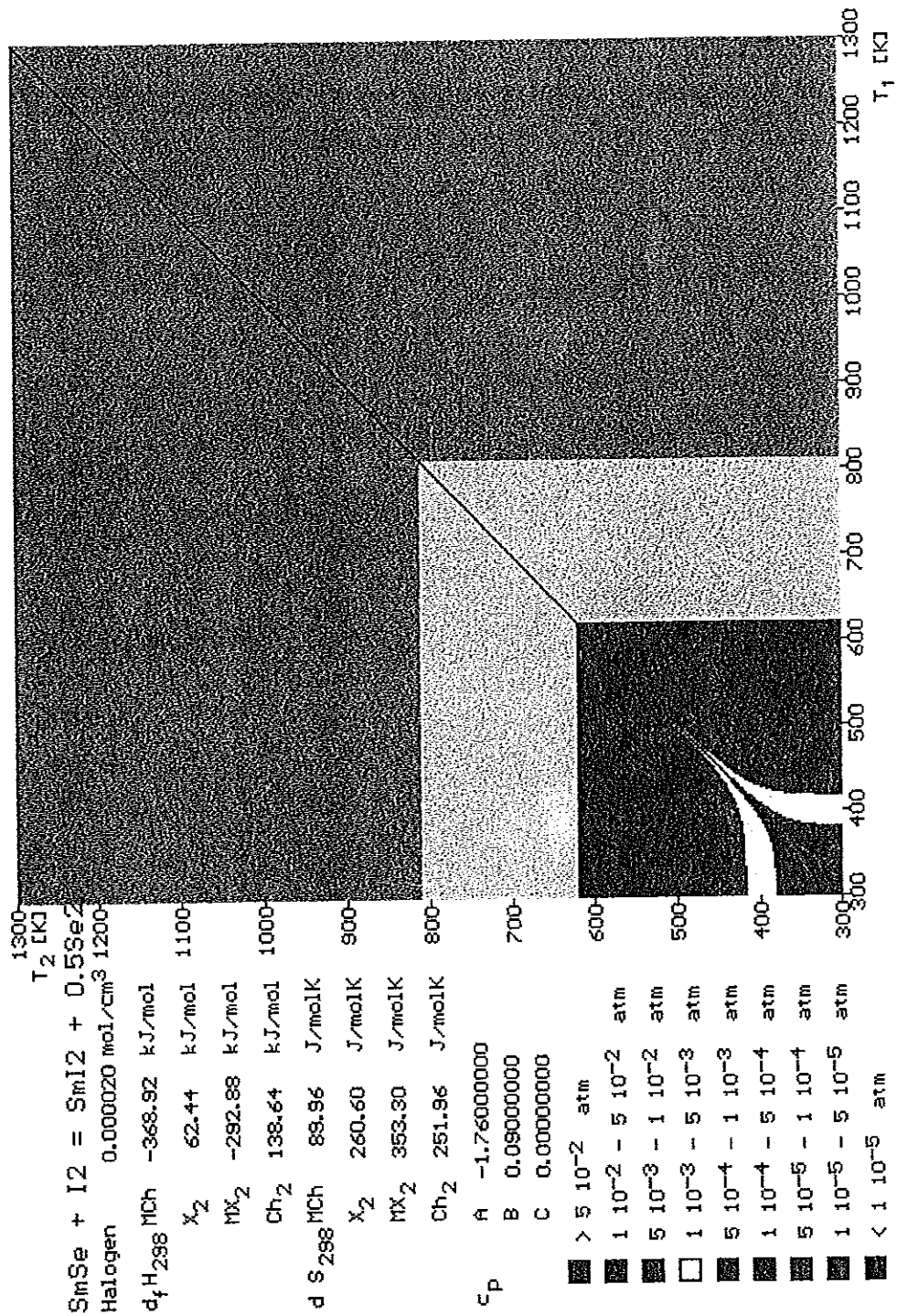
APPENDIX 57-II: SmTe with I₂



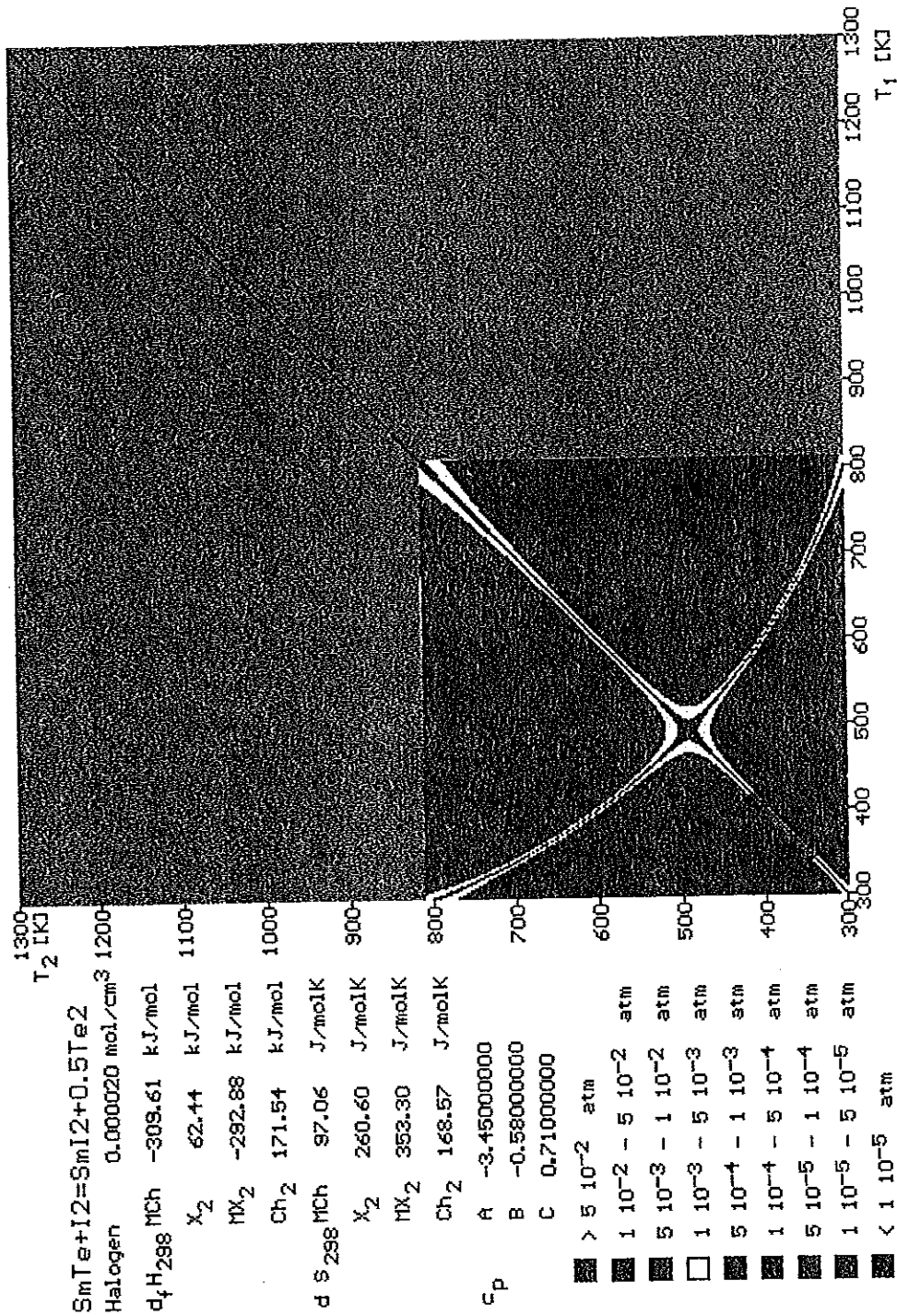
APPENDIX 55-II: SmTe with I_2



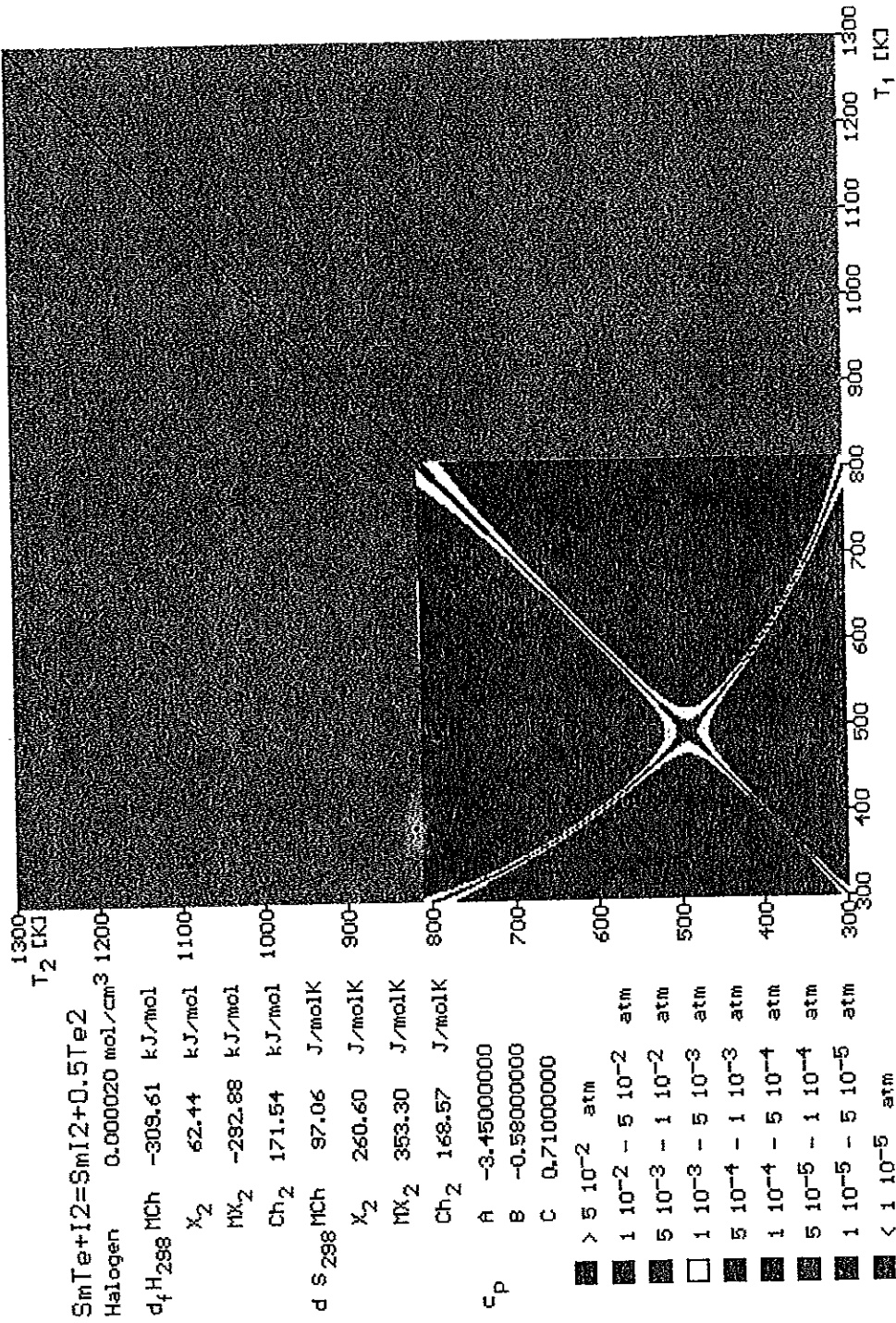
APPENDIX 57-2: SmSe with I_2



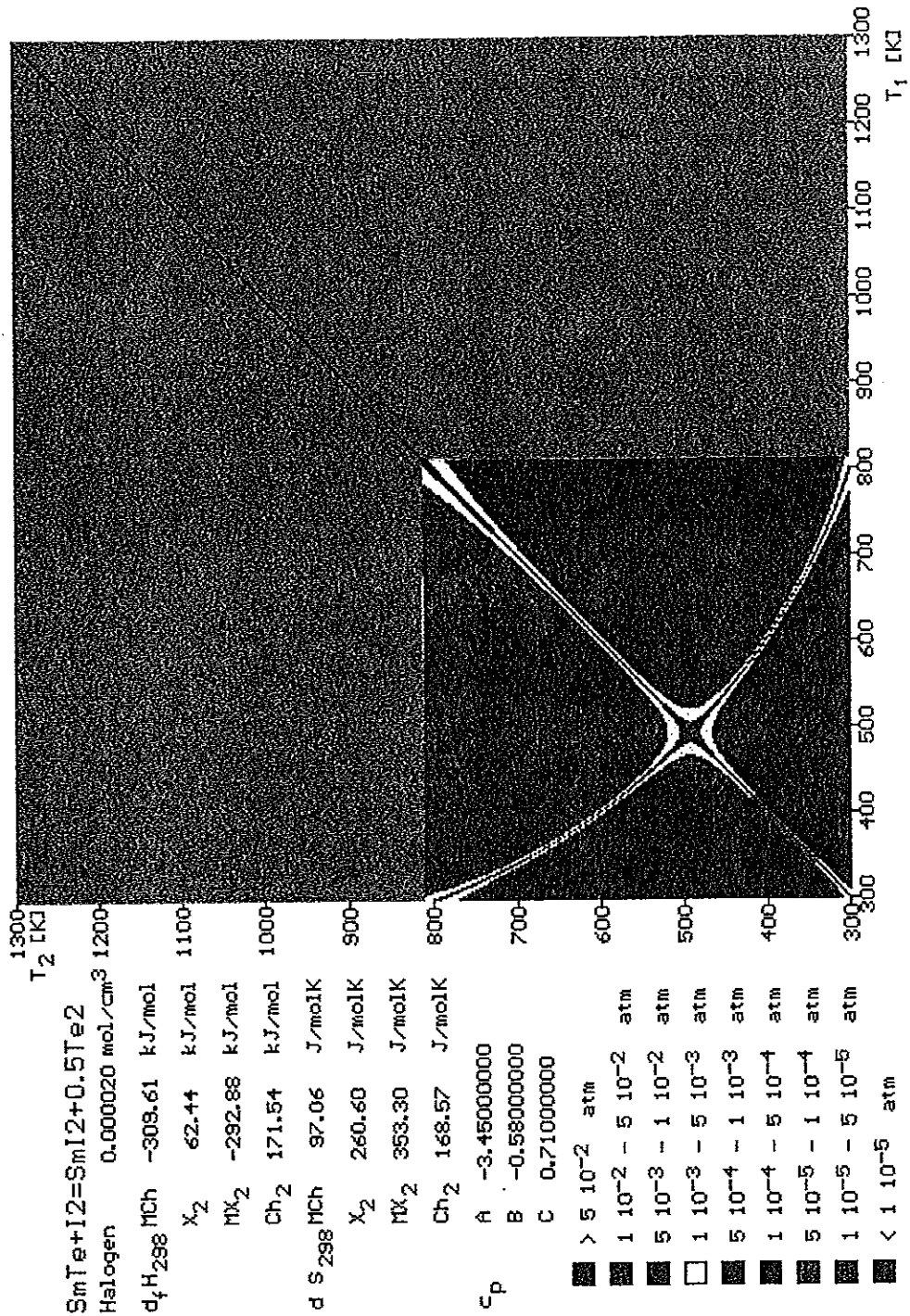
APPENDIX 55-II: SmSe with I₂



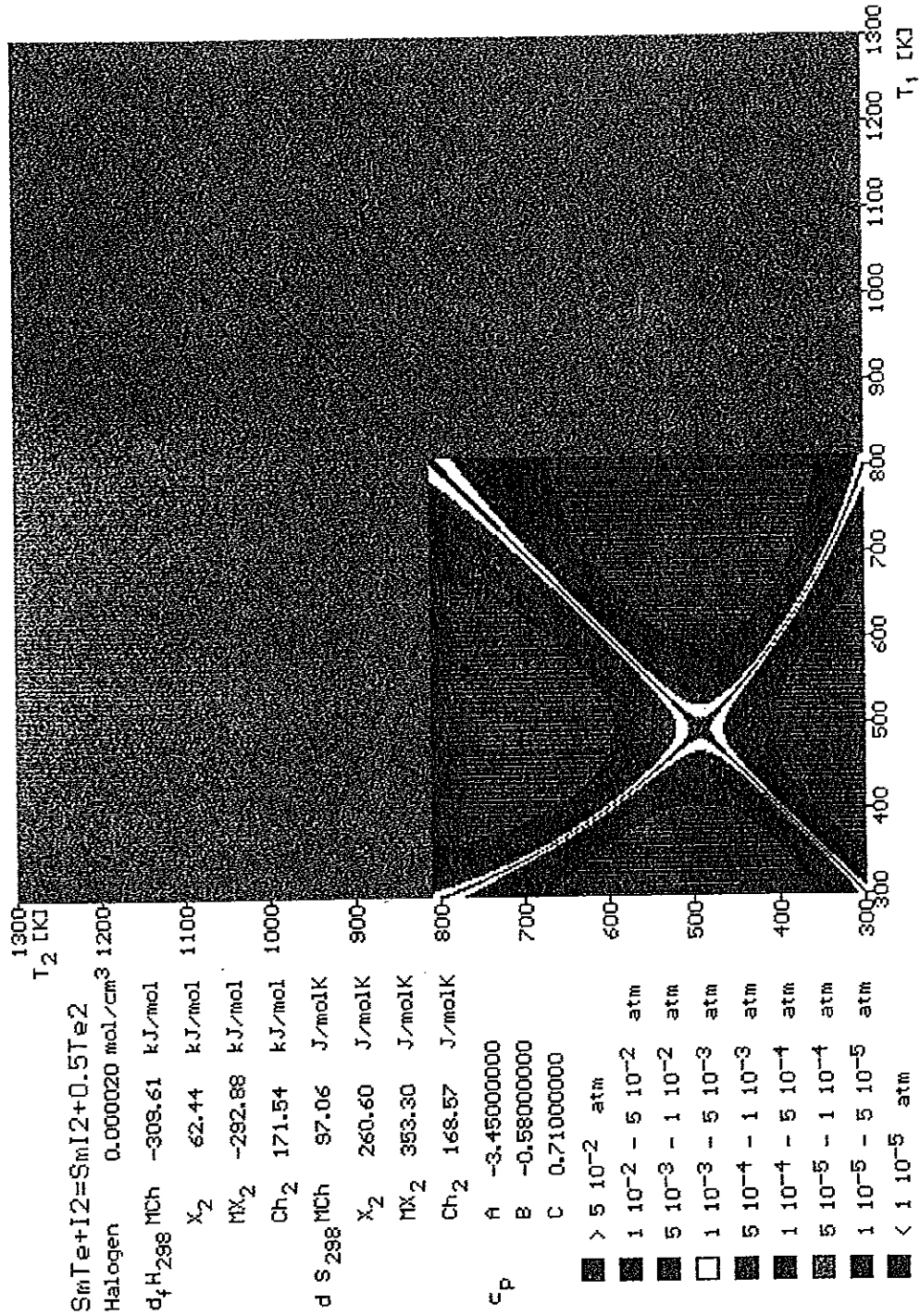
APPENDIX 55-II: SmTe with I₂



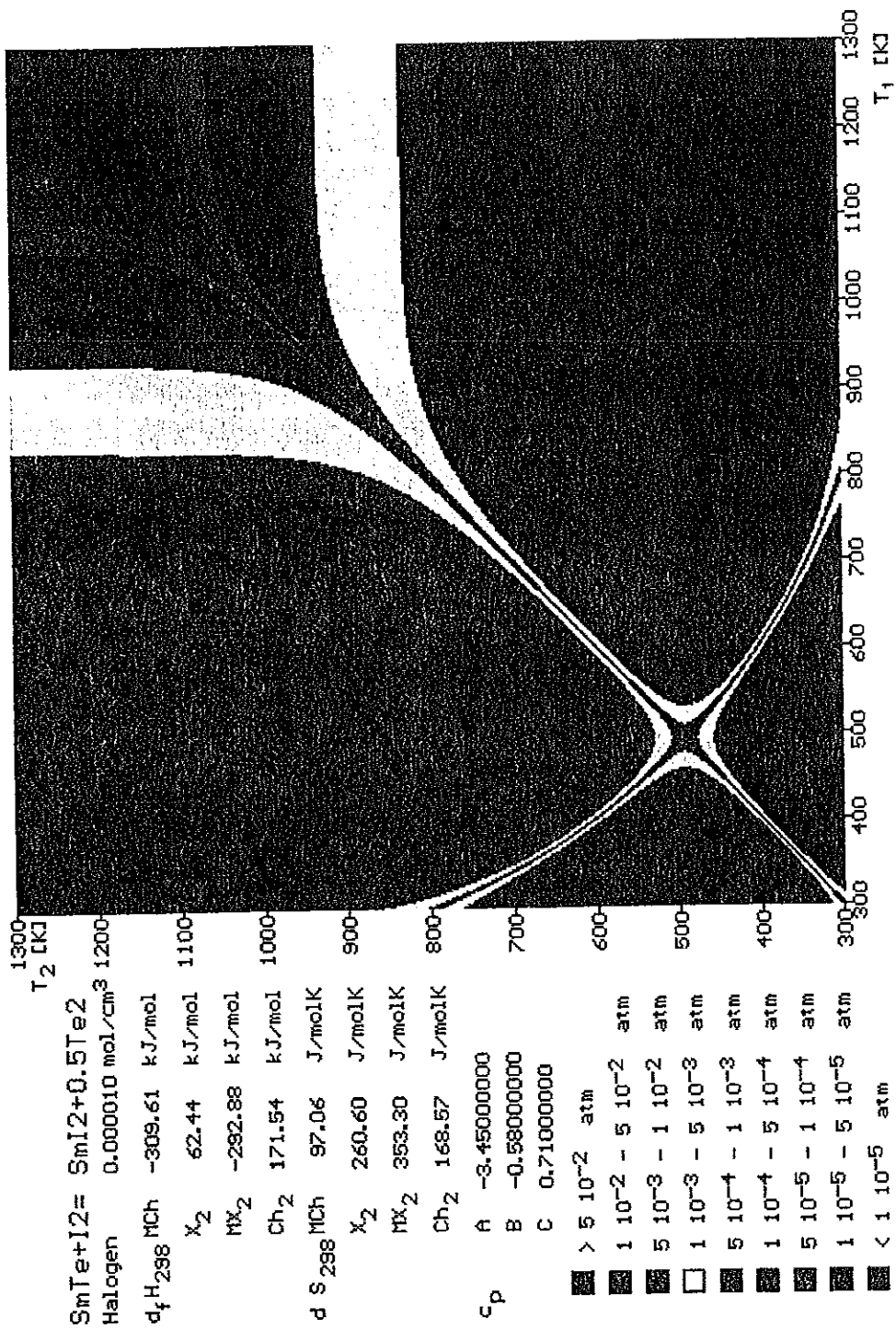
APPENDIX 55-II: SmTe with I₂



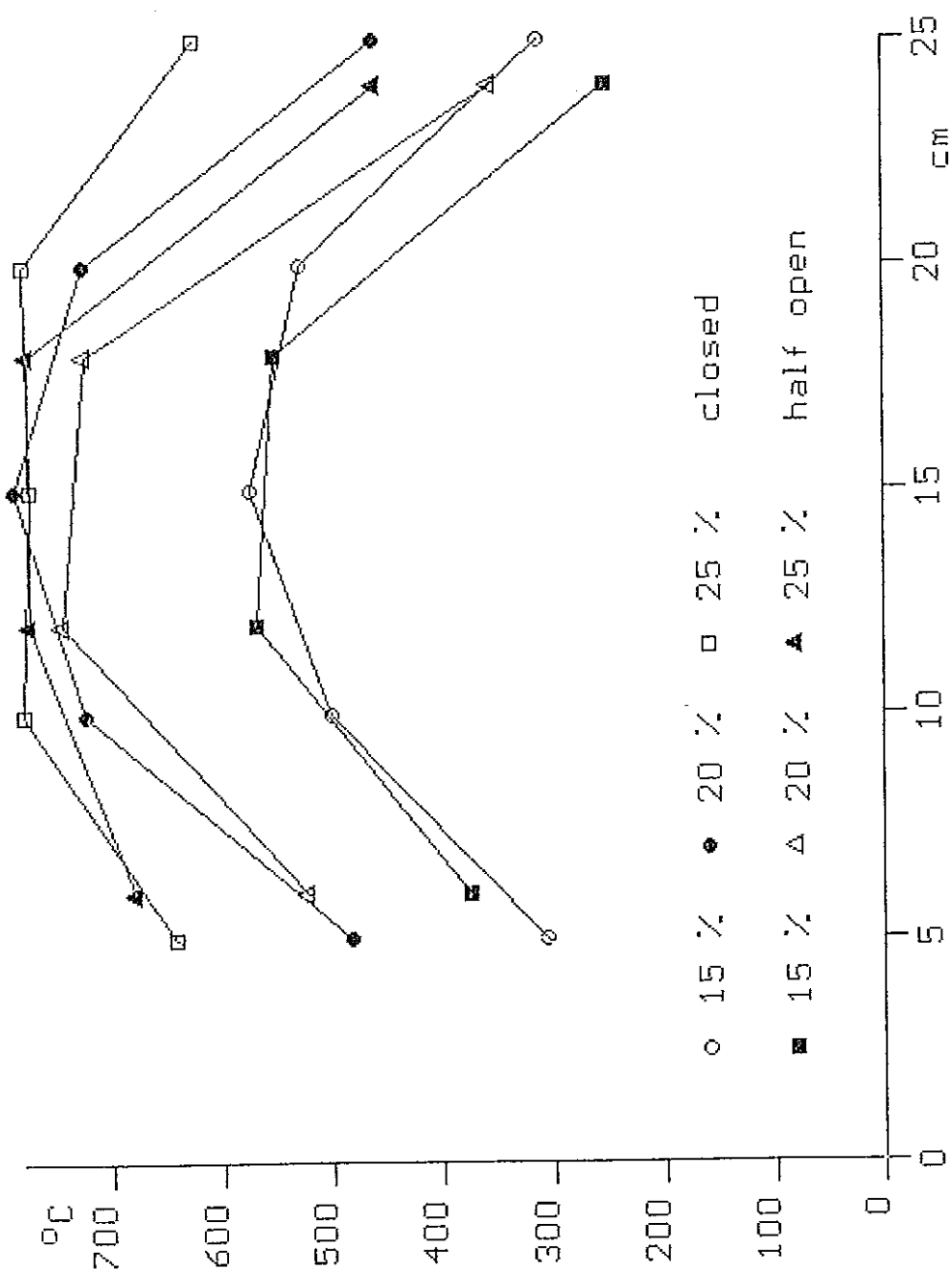
APPENDIX 55-II: SmTe with I₂



APPENDIX 57-II: SmTe with I₂



APPENDIX 55-II: SmTe with I₂



Appendix 57-III: Graph showing the temperature distribution in the furnace in different conditions and various taps.